Sources of tropospheric ozone along the Asian Pacific Rim: An analysis of ozonesonde observations

Hongyu Liu,[1,2] Daniel J. Jacob,[1] Lo Yin Chan,[3] Samuel J. Oltmans,[4] Isabelle Bey,[1,5] Robert M. Yantosca,[1] Joyce M. Harris,[4] Bryan N. Duncan,[1,5] and Randall V. Martin[1]

Received 14 December 2001; revised 8 May 2002; accepted 23 May 2002; published 8 November 2002.

[1] The sources contributing to tropospheric ozone over the Asian Pacific Rim in different seasons are quantified by analysis of Hong Kong and Japanese ozonesonde observations with a global three-dimensional (3-D) chemical transport model (GEOS-CHEM) driven by assimilated meteorological observations. Particular focus is placed on the extensive observations available from Hong Kong in 1996. In the middle-upper troposphere (MT-UT), maximum Asian pollution influence along the Pacific Rim occurs in summer, reflecting rapid convective transport of surface pollution. In the lower troposphere (LT) the season of maximum Asian pollution influence shifts to summer at midlatitudes from fall at low latitudes due to monsoonal influence. The UT ozone minimum and high variability observed over Hong Kong in winter reflects frequent tropical intrusions alternating with stratospheric intrusions. Asian biomass burning makes a major contribution to ozone at <32°N in spring. Maximum European pollution influence (<5 ppbv) occurs in spring in the LT. North American pollution influence exceeds European influence in the UT-MT, reflecting the uplift from convection and the warm conveyor belts over the eastern seaboard of North America. African outflow makes a major contribution to ozone in the low-latitude MT-UT over the Pacific Rim during November–April. Lightning influence over the Pacific Rim is minimum in summer due to westward UT transport at low latitudes associated with the Tibetan anticyclone. The Asian outflow flux of ozone to the Pacific is maximum in spring and fall and includes a major contribution from Asian anthropogenic sources year-round. *INDEX TERMS:* 0322 Atmospheric Composition and Structure: Constituent sources and sinks; 0368 Atmospheric Composition and Structure: Troposphere—constituent transport and chemistry; 0399 Atmospheric Composition and Structure: General or miscellaneous; 0365 Atmospheric Composition and Structure: Troposphere—composition and chemistry; *KEYWORDS:* pollution transport, seasonal variation, case study

Citation: Liu, H., D. J. Jacob, L. Y. Chan, S. J. Oltmans, I. Bey, R. M. Yantosca, J. M. Harris, B. N. Duncan, and R. V. Martin, Sources of tropospheric ozone along the Asian Pacific Rim: An analysis of ozonesonde observations, *J. Geophys. Res.*, *107*(D21), 4573, doi:10.1029/2001JD002005, 2002.

1. Introduction

[2] Ozone in the troposphere is an important greenhouse gas [*Lacis et al.*, 1990]. It is also the primary precursor of OH, the main radical oxidant, and as such plays an essential role in the oxidizing power of the troposphere [*Crutzen*, 1988; *Thompson*, 1992]. In surface air, ozone is a pernicious pollutant and a major constituent of smog. Ozone is produced in the troposphere by photochemical oxidation of hydrocarbons and CO in the presence of NO_x ($NO + NO_2$) radicals, and is also transported down from the stratosphere. Ozone precursors (hydrocarbons, CO, NO_x) are emitted from fossil fuel combustion, industrial processes, biomass burning, vegetation, microbial activity in soils, and lightning. Human activity, including in particular fossil fuel combustion, is a major global source of these precursors.

[3] Tropospheric ozone concentrations have increased since pre-industrial times, at least in the Northern Hemisphere [*Volz and Kley*, 1988; *World Meteorological Organization* (*WMO*), 1994; *Staehelin et al.*, 1994] and are expected to continue to grow in the coming decades as a result of Asian industrialization [*Lelieveld and Dentener*, 2000; *Jonson et al.*, 2001]. There is concern that long-range transport of Asian pollution across the Pacific could elevate background ozone levels in surface air in the United States and undermine the success of domestic strategies for ozone

[1]Department of Earth and Planetary Sciences and Division of Engineering and Applied Sciences, Harvard University, Cambridge, Massachusetts, USA.
[2]Now at Institute for Computer Applications in Science and Engineering, NASA Langley Research Center, Hampton, Virginia, USA.
[3]Department of Civil and Structural Engineering, Hong Kong Polytechnic University, Hong Kong, People's Republic of China.
[4]Climate Monitoring and Diagnostics Laboratory, NOAA, Boulder, Colorado, USA.
[5]Now at Ecole Polytechnique Federale de Lausanne, Lausanne, Switzerland.

0148-0227/02/2001JD002005

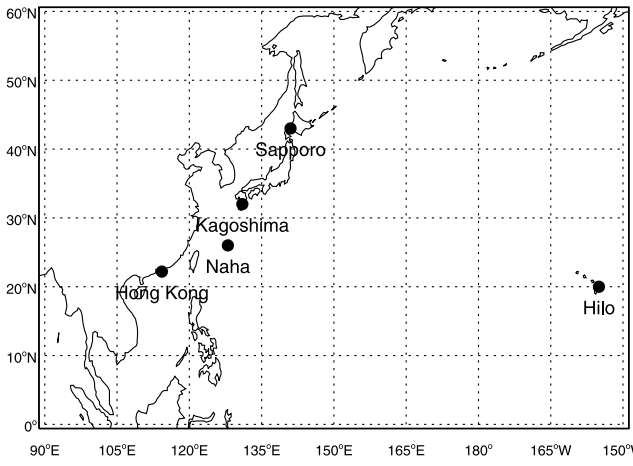

Figure 1. Locations of the five ozonesonde stations analyzed in this study: Hong Kong (22°N, 114°E), Naha (26°N, 128°E), Kagoshima (32°N, 131°E), Sapporo (43°N, 141°E), and Hilo (20°N, 155°W).

smog control [*Jacob et al.*, 1999; *Yienger et al.*, 2000; *Fiore et al.*, 2002]. However, there has been no focused study so far of whether present-day ozone levels measured at the network of ozonesonde stations along the Pacific Rim of the Asian continent [*Logan*, 1999] are consistent with current understanding of tropospheric ozone chemistry. Asian outflow of ozone to the Pacific reflects a complex combination of natural and anthropogenic sources. Understanding quantitatively these contributions in a way that will allow future projections is necessary. In this paper, we use a global three-dimensional chemical tracer model (GEOS-CHEM) [*Bey et al.*, 2001a] driven by assimilated meteorological observations from the Goddard Earth Observing System data assimilation system (GEOS DAS) at the NASA Data Assimilation Office (DAO) to quantify anthropogenic and natural influences on ozone over the Pacific Rim through simulation of the ozonesonde observations in the region. We place a particular focus on Hong Kong (22°N, 114°E) where a new multiyear record of intensive ozonesonde observations is available [*Chan et al.*, 1998; *Liu et al.*, 1999].

[4] Figure 1 shows the locations of the five ozonesonde stations examined in this study. The four stations along the Asian Pacific Rim are spread from 22°N to 43°N. The Hong Kong data are of particular importance because tropospheric ozone observations in Southeast Asia are otherwise scarce (see review by *Chan et al.* [1998]). The most extensive observations are from the Japanese ozonesonde stations, which have been operational for over 30 years (Kagoshima, 32°N, 131°E; Tateno, 36°N, 140°E; Sapporo, 43°N, 141°E) or 10 years (Naha, 26°N, 128°E). Tateno is not included in this study since the observations in the lower troposphere are influenced by proximity to Tokyo [*Logan*, 1999]. The seasonal cycle at the Japanese stations shows a summer minimum in the lower troposphere (LT) at low latitudes due to monsoonal intrusion of low-ozone air from the tropical Pacific, and a broad spring/summer maximum in the middle troposphere (MT)-upper troposphere (UT) at midlatitudes which is a common feature in the Northern Hemisphere [*Logan*, 1985, 1999]. Ozone trends at the Japanese stations for 1970–1991 show a significant increase of <1% per year at 500 hPa with larger increases at lower altitudes (~2% per year in the planetary boundary layer), but with no significant trend above 500 hPa [*Logan*, 1994; *Akimoto et al.*, 1994; *Lee et al.*, 1998; *Oltmans et al.*, 1998]. The trend in the boundary layer may reflect the increasing emission of ozone precursors from East Asia [*Akimoto et al.*, 1994; *Lee et al.*, 1998].

[5] The Hong Kong Observatory (HKO) has performed monthly ozonesonde soundings since October 1993 [*Shun and Leung*, 1993; *Yeung et al.*, 1996]. Between September 1995 and April 1997, weekly or more frequent ozonesonde soundings were carried out as a joint venture by the Hong Kong Polytechnic University and HKO. As a result of these efforts, a total of 152 ozonesonde profiles were obtained (Table 1). The tropospheric ozone column has a maximum in spring and a minimum in summer [*Chan et al.*, 1998]. Downward transport of ozone from the stratosphere contributes to the spring maximum in the UT, but in the lower free troposphere the spring maximum is due to biomass burning in Southeast Asia [*Liu et al.*, 1999]. The seasonal cycle of ozone below 2 km is biomodal with ozone peaks in spring and fall, both resulting from photochemical buildup of ozone. The higher value in fall reflects the building continental high pressure system and high solar radiation, compared to cloudy and humid weather in spring [*Chan et al.*, 1998; *Lam et al.*, 2001; *Wang et al.*, 2001]. The Hong Kong data also show an ozone minimum in the UT in late fall and winter, reflecting tropical influence [*Chan et al.*,

Table 1. Number of Ozonesonde Soundings

Station	Latitude	Longitude	Years Used in Analysis[a]	Month											
				J	F	M	A	M	J	J	A	S	O	N	D
Hong Kong	22°N	114°E	1993										1	0	3
			1994	1	6	2	3	0	1	1	0	1	1	1	1
			1995	1	1	1	1	1	1	1	1	4	2	4	5
			1996	9	5	9	18	5	3	7	5	3	5	5	12
			1997	7	2	3	3								
Naha	26°N	128°E	9/89–12/95	16	11	14	16	17	12	15	13	16	19	16	20
			1996	5	4	1	2	2	1	3	4	3	5	3	4
Kagoshima	32°N	131°E	1/80–12/95	20	21	23	18	19	15	14	9	19	26	21	22
			1996	4	4	2	4	4	2	2	5	4	4	4	4
Sapporo	43°N	141°E	1/80–12/95	20	20	19	23	28	16	13	18	23	26	19	25
			1996	2	6	3	4	3	2	3	3	4	3	2	4
Hilo	20°N	155°W	1/85–12/93	31	30	27	28	28	29	26	36	31	35	28	29
			1996	3	3	2	3	5	3	5	4	4	4	3	3

[a] Ozonesonde data for Japanese stations and Hilo are taken from *Logan* [1999] and the World Ozone and Ultraviolet Data Center (WOUDC).

1998]. More recently, *Chan et al.* [2001] reported the influence of unusually large Indonesian forest fires on tropospheric ozone at Hong Kong in December 1997.

[6] We describe briefly in section 2 the ozonesonde measurements and the models used in this paper. The seasonal cycle of ozone is presented in section 3. Transport of ozone pollution over the Pacific Rim is described in section 4. In section 5, we investigate contributions to ozone from different sources. We present some case studies in section 6 and discuss implications for the Asian outflow of ozone to the Pacific in section 7, followed by summary and conclusions in section 8.

2. Data and Methods

[7] Routine balloon-borne ozonesonde soundings began at HKO in October 1993 [*Shun and Leung*, 1993]. The ozone sensor is the Electrochemical Concentration Cell (ECC) and the radiosonde is of the model RS80 403 MHz Vaisala. The soundings are regularly made at 1400 local time (06 UTC) at HKO King's Park Meteorological Station, an urban site 66 m above mean sea level. Part of the data set was used in previous studies [*Chan et al.*, 1998, 2000; *Liu et al.*, 1999].

[8] Ozonesonde data for other sites in Table 1 are taken from *Logan* [1999], who obtained the original data from various sources, in particular, the World Ozone and Ultraviolet Data Center, Environment Canada, Downsview, Ontario (http://www.tor.ec.gc.ca/woudc). Ozone concentrations were given at 22 pressure levels from 1000 to 10 hPa and the profiles were scaled to the Dobson or Brewer total ozone. Sonde launches at Japanese stations are scheduled at around 06 UTC, while the schedule at Hilo varies.

[9] Backward air trajectories are computed with the CMDL (Climate Monitoring and Diagnostic Laboratory) 10-day isentropic back trajectory model [*Harris and Kahl*, 1994], which uses gridded analysis produced by the European Center of Medium Range Weather Forecasts (ECMWF). Trajectories are calculated twice daily, at 0000 and 1200 UT arrival times.

[10] Global simulation of ozone for the 1995–1997 period is conducted with the GEOS-CHEM global 3-D model of tropospheric chemistry [*Bey et al.*, 2001a] driven by GEOS DAS assimilated meteorological observations. The simulation presented here uses GEOS-CHEM version 4.6 (http://www-as.harvard.edu/chemistry/trop/geos/) and the GEOS1-STRAT meteorological observations for December 1995 to January 1997. Reference will also be made to simulations conducted for other years (1991–1997) and presented in other papers [*Bey et al.*, 2001b; *Fiore et al.*, 2002; *Li et al.*, 2001, 2002; *Chandra et al.*, 2002; *Martin et al.*, 2002]. The GEOS1-STRAT data have a horizontal resolution of 2° latitude by 2.5° longitude, and 46 vertical sigma levels (of which 23 are always above the tropopause). The midpoints of the lowest four levels are at ~50, 250, 600, and 1100 m above the surface. We retain the 23 tropospheric layers from GEOS1-STRAT in the GEOS-CHEM model but merge the upper 23 stratospheric layers into just 3 sigma levels. We use in general a degraded horizontal resolution (4° latitude by 5° longitude) for computational expediency. For some case studies (section 6), the original 2° × 2.5° model resolution is used to better resolve features of transport. The model uses the advection scheme of *Lin and Rood* [1996] and the moist convective mixing scheme of *Allen et al.* [1996]. Rapid vertical mixing within the GEOS-diagnosed mixed layer is assumed. The Synoz (synthetic ozone) scheme [*McLinden et al.*, 2000] is used as a flux upper boundary condition for ozone in the stratosphere and yields a cross-tropopause ozone flux of 475 Tg yr^{-1}.

[11] The model solves the chemical evolution of 80 chemical species with a fast Gear solver [*Jacobson and Turco*, 1994] and transports 24 chemical tracers to describe tropospheric O_3-NO_x-hydrocarbon chemistry. Emissions and deposition are mostly as described by *Bey et al.* [2001a]. The 1995 anthropogenic emission for Asia (0–60°N, 65–150°E) is 7.4 Tg N yr^{-1} for NO_x and 135.8 Tg yr^{-1} for CO. The reader is referred to *Bey et al.* [2001a, 2001b] for the anthropogenic emissions in other geopolitical regions. The global lightning source is 3 Tg N yr^{-1}. The present version includes an improved biomass burning emission inventory with seasonal variability constrained by satellite observations [*Duncan et al.*, 2002], but with no interannual variability. A summary of the biomass burning emissions for various regions of the globe is given by *Duncan et al.* [2002]. Biomass burning over continental Southeast Asia lasts from December to May and peaks in March, while biomass burning in northern Africa begins in October and peaks in December through March.

[12] General evaluations of the GEOS-CHEM simulation of tropospheric O_3-NO_x-hydrocarbon chemistry have been presented by *Bey et al.* [2001a]. The model captures well the main features of tropospheric ozone. It simulates correctly the seasonal phases (generally to within a month) and amplitudes (generally to within 10 ppbv) for different regions and altitudes, although it underestimates the seasonal amplitude at northern midlatitudes. The model has been applied previously to study tropospheric ozone and its precursors over the western Pacific [*Bey et al.*, 2001b], in the Middle East [*Li et al.*, 2001], over the United States [*Fiore et al.*, 2002], over the Atlantic [*Li et al.*, 2002], and in the tropics [*Chandra et al.*, 2002; *Martin et al.*, 2002]. The simulation of convective transport and scavenging with the GEOS data has also been evaluated independently using chemical tracers [*Allen et al.*, 1996; *Liu et al.*, 2001; *Bell et al.*, 2002].

[13] Simulation of the PEM-West B aircraft mission (February–March, 1994) by *Bey et al.* [2001b] indicates that the model reproduces well the latitudinal and vertical distribution of the Asian outflow of ozone and NO_y species over the western Pacific. This study found that although boundary layer outflow of Asian pollution is largely restricted to high latitudes (north of 35°N), the maximum outflow of Asian pollution is in the lower free troposphere at ~25–30°N. It also identified significant contributions to the Asian outflow from European anthropogenic emissions in the LT at high latitudes and from African biomass burning emissions in the UT at low latitudes.

[14] Our simulation is conducted for the December 1995 to January 1997 period, with a 5-month prior period (July–November) for initialization. Results for 1996–1997 are used for analysis. In comparison to ozonesonde observations, the model is sampled at the actual sounding time unless stated otherwise. To identify source regions in the

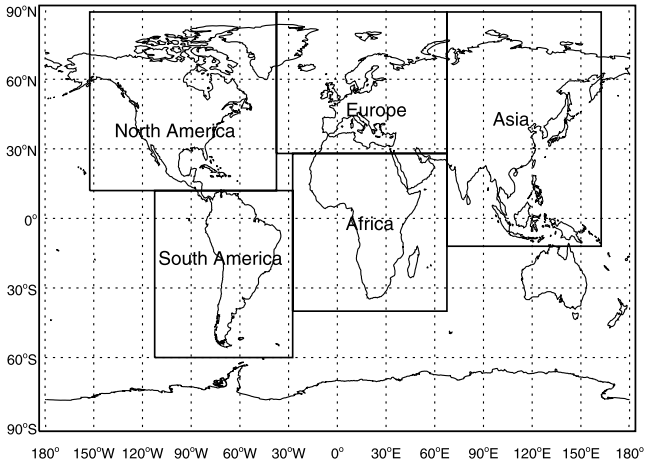

Figure 2. Tropospheric source regions used for tagged tracer simulations.

model, we decompose ozone (actually odd oxygen or O_x) and CO into tagged tracers where tagging indicates different source regions. This approach has been used previously by *Wang et al.* [1998] for ozone and *Bey et al.* [2001b] and *Staudt et al.* [2001] for CO. Figure 2 shows the tropospheric source regions used in this study for the tagged tracer simulations. Ozone produced in the stratosphere is tagged as a separate tracer. The sum of tagged tracers for all source regions replicates closely the results from the standard full-chemistry simulation.

[15] It should be stressed that tagging ozone by source region does not actually describe the sensitivity of ozone to emissions in that region because of chemical non-linearity. We also conduct sensitivity simulations where emissions from a given source type or region are suppressed. All sensitivity simulations are conducted for the same period and with the same initialization as for the standard simulation.

3. Seasonal Variation of Ozone Along the Pacific Rim

[16] Figure 3 compares simulated and observed daily ozone concentrations averaged over three altitude bands (850–700, 700–300, and 300–120 hPa) at Hong Kong in 1996. (A similar comparison using monthly averaged values is shown in Figure 4a.) A total of 86 ozonesonde launches were made during the year with intensive launches during winter and spring (Table 1). The observed seasonal pattern is similar to that reported by *Chan et al.* [1998] for October 1993 to August 1996. Concentrations peak in spring and are minimum in the LT in summer. There is also a minimum in the UT (300–100 hPa) in late fall and winter. As mentioned earlier, high ozone concentrations in the LT (~700 hPa) in spring are due to Southeast Asian biomass burning [*Liu et al.*, 1999]. In summer and fall, high-ozone episodes occasionally occur in the MT-UT. Considerable variability is seen in both the observations and the model.

[17] The model generally reproduces the observed ozone concentrations over Hong Kong, with mean biases of + 5.2 ppbv (8%), + 3.0 ppbv (5%), + 6.8 ppbv (15%) in the UT, MT, and LT, respectively (Figure 3). The bias in the LT may be due to titration of ozone in the observations by recently emitted nitric oxide from heavy local traffic [*Yeung et al.*, 1996]. The model reproduces 40% of the day-to-day variability of ozone in the UT (R = 0.65), with a larger percentage (56%) in January–April. In the MT/LT, the correlations between the model and the observations are weaker (R = 0.32 in MT and 0.38 in LT). The stronger correlation in the UT reflects larger variability of ozone. The model reproduces the spring maximum from biomass burning and stratospheric influence, the summer minimum from the monsoon circulation, and the minimum in the UT in winter. While the model reproduces ozone episodes in the MT-UT in October/November, it misses the early August ozone episode. The model does not capture the relatively low ozone values in the UT during September when air masses frequently have an origin over the western Pacific. It also overestimates the MT ozone in early December, but ozone concentrations sampled in an adjacent southern grid box in the model are close to the observations.

[18] Ozonesonde observations at Japanese stations in 1996 are limited (Table 1). In Figures 4b–4d we compare the model simulation for 1996 (right column) with the ozonesonde climatology (left column) given by *Logan* [1999]. The mature phase of cold ENSO (El Nino and the

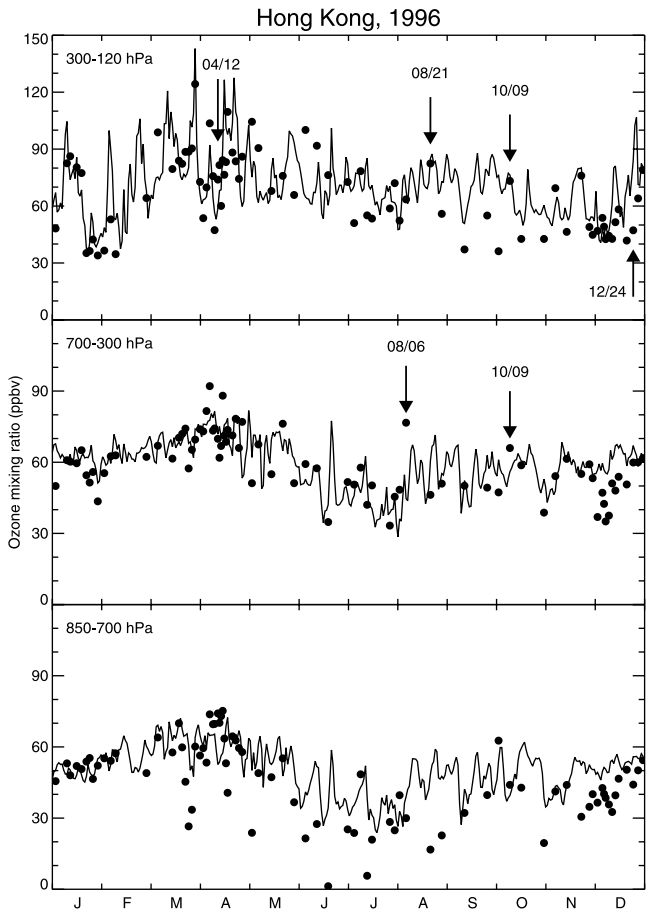

Figure 3. Seasonal variation of ozone over Hong Kong in 1996 averaged over three altitude bands (850–700, 700–300, and 300–120 hPa). Model results (solid line) are compared to observations (dots). Arrows indicate the events analyzed in the case studies (section 6).

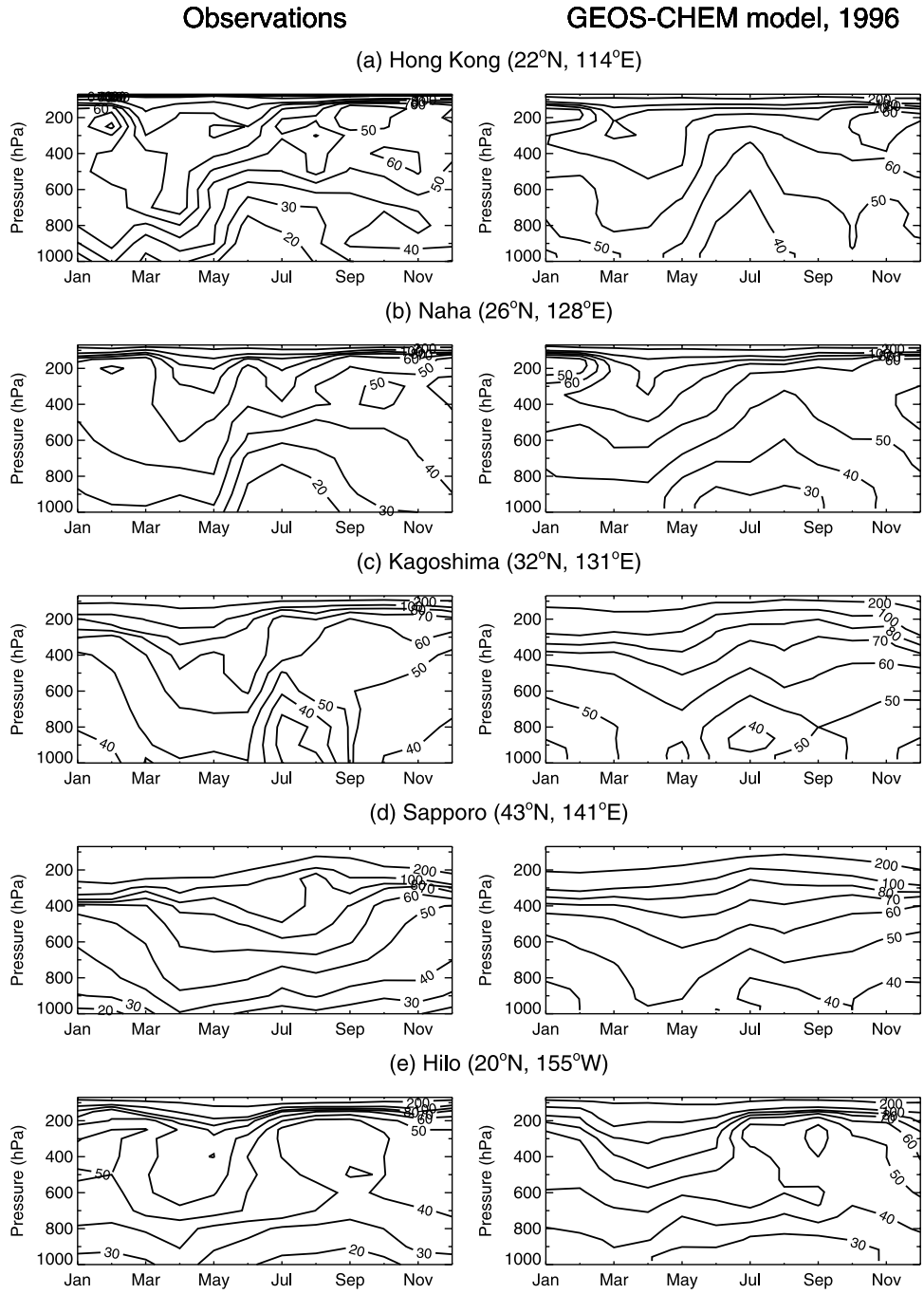

Figure 4. Seasonal variation of ozone concentrations (ppbv) as a function of altitude for the ozonesonde sites of Figure 1. Observations (left panels) are compared to model results for 1996 (right panels). The observations at Hong Kong are for 1996 while the observations at the other sites are from a long-term climatology (Table 1). All values are monthly averages. Contour levels are 20, 30, 40, 50, 60, 70, 80, 100, and 200 ppbv.

Southern Oscillation) conditions (La Nina) characterizes the climate of 1996, when both the subtropical Hadley circulation and the East Asian jet are enhanced (in particular during December 1995–May 1996) [*Halpert and Bell*, 1997]. This may contribute to the discrepancies between the model results for 1996 and the ozonesonde climatology. Combining model simulations for 1996 with those for other years (1991–1995, 1997), we find that the wintertime UT ozone minimum at low latitudes (Hong Kong and Naha) is more apparent (~5–10 ppbv lower in value) and frequently seen during the cold phase relative to the warm phase, due to enhanced intrusion of tropical air. Nevertheless, the overall pattern of seasonal variation in the model is similar between years at the ozonesonde stations analyzed here.

[19] The seasonal cycle of ozone over Naha is similar to that for Hong Kong, with a spring maximum and a summer minimum (Figure 4b). As latitude increases, the ozone maximum in the MT/UT shifts from spring at Naha

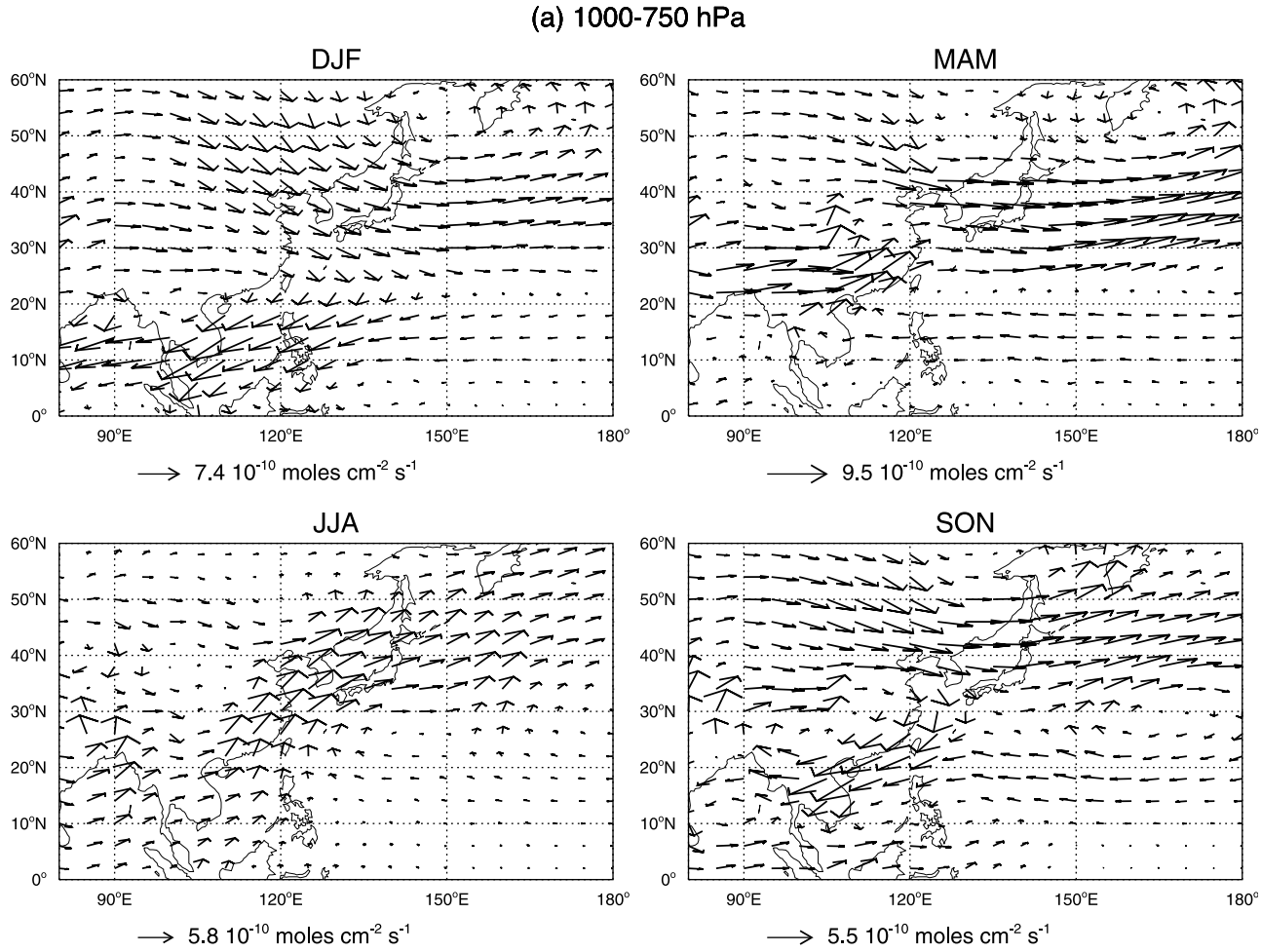

Figure 5. Horizontal fluxes of ozone produced in the Asian troposphere, shown for (a) 1000–750 hPa column, (b) 500 hPa, and (c) 200 hPa. Values are seasonal model averages for 1996.

(26°N) to summer at Sapporo (43°N) [*Logan*, 1999]. The monsoonal summer minimum is more pronounced at lower altitudes and latitudes. The simulated vertical distribution of ozone and its seasonal variation at Naha are consistent with the ozonesonde climatology (Figure 4b) and similar to those at Hong Kong (Figure 4a), but the model does not fully capture the summer minimum in the LT at these sites. The model simulates a weaker enhancement of ozone in the LT in spring at Naha than at Hong Kong, due to the higher latitude and thus lesser influence from Southeast Asian biomass burning, but the observations at Naha are too sparse to test this result. The UT wintertime minimum in the Naha climatology is less pronounced than in the Hong Kong data or model results for 1996, due to enhanced intrusion of tropical air in 1996 as mentioned above. The decreasing magnitude of the summer minimum with latitude and altitude reflects in the model the weakening of the monsoonal influence. The shift of the ozone maximum in the MT-UT from spring at Naha to summer at Sapporo is a result of increased photochemical production of ozone at northern midlatitudes in summer. The simulations at Kagoshima and Sapporo (Figures 4c and 4d) illustrate the slight tendency for the model to underestimate the amplitude of the observed seasonal variation in the MT-UT at northern midlatitudes [*Bey et al.*, 2001a].

[20] At Hilo, model and observations show a spring maximum and a late summer minimum above 500 hPa (Figure 4e). The former is explained by a combination of stratospheric influence and Asian pollution outflow [*Wang et al.*, 1998; *Kentarchos et al.*, 2001]. The latter is in contrast with the seasonality of ozone at the stations along the Pacific Rim and is associated with convective activity in the wet season which mixes ozone-poor air from the marine boundary layer where photochemistry provides a net sink for ozone [*Oltmans et al.*, 1996].

4. Transport of Ozone Pollution Along the Pacific Rim

[21] We use here a tagged ozone simulation to describe the transport pathways for ozone photochemically produced in the Asian troposphere and thus help our understanding of sources of tropospheric ozone along the Asian Pacific Rim. Figure 5 shows the seasonally averaged horizontal fluxes of ozone produced in the Asian troposphere for the 1000–750 hPa column (Figure 5a), 500 hPa (Figure 5b), and 200 hPa (Figure 5c). The large fluxes in the MT-UT reflect strong winds in this part of the troposphere. In winter, the Asian pollution is kept within the boundary layer by the general subsidence over the Asian continent. The northwesterly

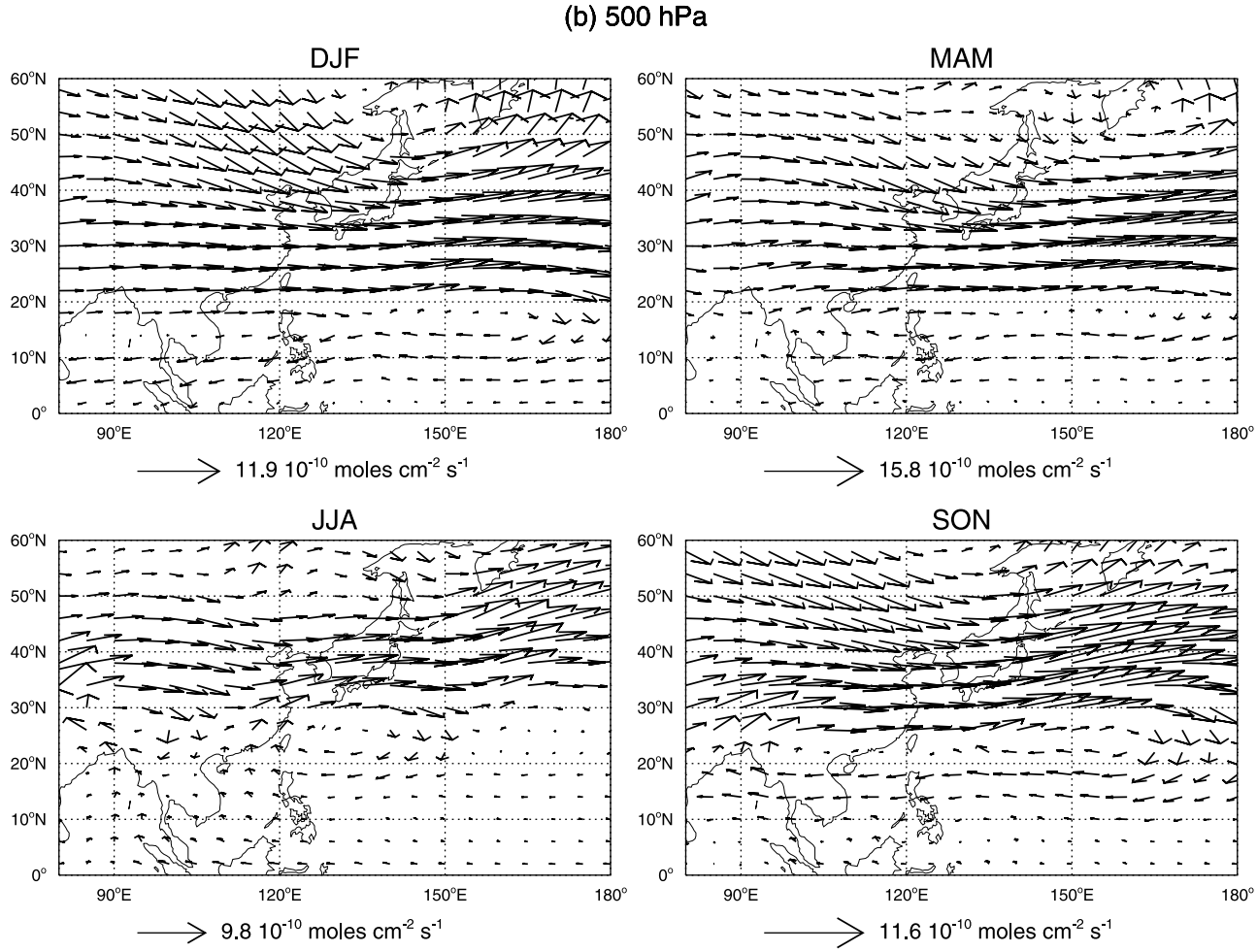

Figure 5. (continued)

(>25°N) and northeasterly monsoons (<25°N) sweep this pollution south toward the tropics, where photochemical production of ozone is active, as reflected by the large ozone fluxes shown in Figure 5a (DJF). The pollution is subsequently lifted up into the UT by deep convection over the maritime continent, from where it is transported northward along the upper-branch of the local Hadley circulation and into the mid- latitude westerlies (Figure 5c). In this way, Asian pollution influences the global ozone budget in winter, as previously suggested by *Newell et al.* [1997]. As shown below in section 6, ozone production due to tropical lightning NO_x emissions also contributes significantly to the Asian outflow of ozone in the wintertime UT.

[22] In summer, the monsoonal flow transports Asian ozone pollution along the Pacific Rim towards the northeast (Figure 5a) and the pollution is then subject to frequent lifting into the UT by convection; this is discussed further in the next section. While part of this pollution in the UT is transported eastward to the northern Pacific, a large fraction circulates southward and then westward around the so-called Tibetan anticyclone (South Asia high), eventually reaching the Middle East [*Li et al.*, 2001]. The Tibetan anticyclone is a climatological feature of the UT circulation over eastern Asia in summer and is characterized by southward transport along the eastern Asia coast, as contrasted to the southwest monsoonal flow in the LT, and westward transport at low latitudes as part of the tropical easterly jet [*Ding*, 1994; *Ye and Wu*, 1998], as shown in Figure 5c. In the MT, the Tibetan anticyclone is much weaker and located further west (Figure 5b), and Asian pollution is transported to the Pacific around the northern flank of the subtropical western Pacific high.

[23] Spring and fall are transitional meteorological periods. Outflow of Asian pollution to the Pacific in spring is discussed in detail by *Bey et al.* [2001b]. This outflow is driven by cold fronts sweeping across eastern Asia [*Yienger et al.*, 2000], and is maximum in the lower free troposphere at ~25–30°N following frontal lifting [*Bey et al.*, 2001b]. Convective transport to the UT of ozone pollution from biomass burning also makes a major contribution to Asian outflow at lower latitudes. In fall, a prominent feature is the southwest transport of ozone in the boundary layer along the South China coast where photochemistry is quite active in this season [*Wang et al.*, 2001]. This is in contrast to the northeast transport in spring in the same region.

5. Sources of Ozone Along the Pacific Rim

[24] We examine in this section for different seasons of 1996 the relative contributions to tropospheric ozone along the Pacific Rim from different source types and source

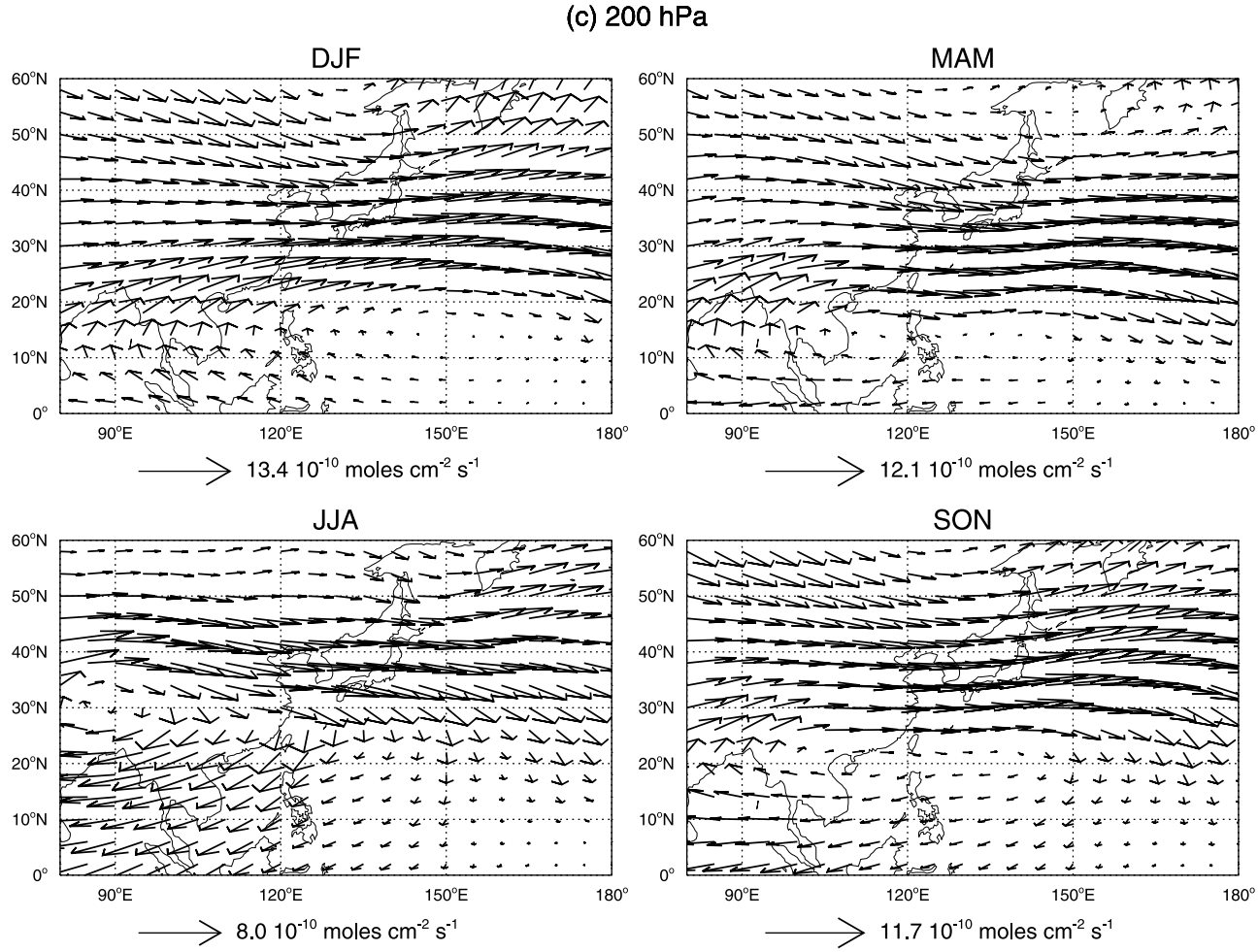

Figure 5. (continued)

regions. Figure 6 shows the contributions to ozone at Hong Kong from chemical production in the Asian and African troposphere and in the stratosphere, as determined from tagged tracers (section 3). Figure 7 shows the changes in ozone concentrations at Hong Kong when Asian fossil fuel, African biomass burning, or lightning emissions are suppressed, as determined from sensitivity simulations. Similar plots were constructed for other source regions and source types, and also for the other stations in Figure 1. They provide the context for the source analysis that follows.

5.1. Asian Pollution and Biomass Burning

[25] A large fraction of ozone in the free troposphere along the Asian Pacific Rim is produced within Asia, in particular in summer because of the generally stronger convective mixing of ozone and its precursors (see Figure 6a and Figure 7a for Hong Kong). In summer, unusually strong photochemical production of ozone (6–10 ppbv/day) occurs in the UT over the eastern Asia coast and the Indian subcontinent. While the former is explained by rapid convective transport of ozone precursors from the continental boundary layer along the East Asia coast [*Berntsen et al.*, 1996; *Mauzerall et al.*, 2000], the latter is mostly due to lightning emissions over northern India and the Indochina peninsula [*Li et al.*, 2001].

[26] In the LT over Hong Kong, Asian pollution influence exhibits a biomodal seasonal behavior with maxima in spring and fall (Figure 7a), consistent with our previous analysis of ozonesonde observations below 2 km [*Chan et al.*, 1998] and previous surface observations along the China coast [*Chameides et al.*, 1999; *Luo et al.*, 2000; *Lam et al.*, 2001; *Wang et al.*, 2001]. We find a larger influence from Asian pollution in fall than in spring, again consistent with observations [*Lam et al.*, 2001]. Prevailing clear skies over southern China in fall, reflecting the building high pressure system over the Asian continent, promote photochemical activity in the region [*Chan et al.*, 1998; *Wang et al.*, 2001]. The biomodality of Asian pollution influence is also seen in the model at Naha and Kagoshima, but is not present at Sapporo where maximum pollution influence is centered in late spring and summer.

[27] High ozone of Asian origin in the springtime (March) LT over Hong Kong (Figure 6a) reflects strong influences from Southeast Asian biomass burning. Figure 8 (bottom panel) shows the monthly averaged decreases in 700 hPa ozone concentrations for March when Southeast Asian biomass burning emissions are suppressed, relative to the standard simulation. The effect is important at Hong Kong and to a lesser extent at Naha, and decreases as latitude increases. Through convective lifting, Southeast

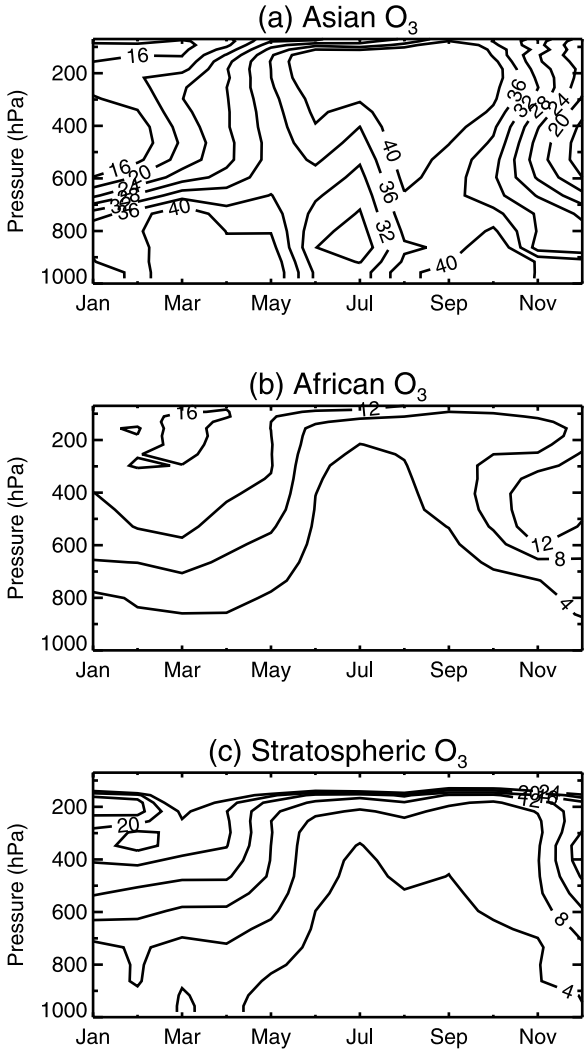

Figure 6. Major source regions for ozone at Hong Kong as a function of altitude and season in 1996. The plots show model results for tagged ozone (a) produced in the Asian troposphere, (b) produced in the African troposphere, and (c) transported from the stratosphere. Values are monthly averages. Contour levels are 4, 8, 12, 16, 20, 24, 28, 32, 36, and 40 ppbv.

Asian biomass burning also has an effect on UT ozone over South China and the western Pacific (Figure 8, upper panel). The Asian contribution to ozone over Hilo is mainly seen in the free troposphere in late spring (April–June) and is much weaker than at the Pacific Rim sites. Seasonal biomass burning is also known to make a major contribution to Asian outflow of CO and hydrocarbons over the western Pacific in spring [*Blake et al.*, 2001; *Staudt et al.*, 2001; *Bey et al.*, 2001b].

5.2. European Pollution

[28] Figure 9a shows seasonally averaged decreases in 900 hPa ozone concentrations for spring and fall in a sensitivity simulation where European anthropogenic emissions are suppressed, relative to the standard simulation. In winter, the Siberian anticyclone promotes transport of European pollution to the Pacific Rim [*Newell and Evans*, 2000], but production of ozone is slow. In summer, European influence on the Pacific Rim is minimum throughout the troposphere because of the Asian monsoon. Maximum influence (still less than 5 ppbv) is in spring below 4-km altitude at the high-latitude stations when favorable transport is combined with active photochemistry.

5.3. North American Pollution

[29] While maximum European pollution influence occurs in the LT in spring, maximum North American pollution influence is in the UT in fall (Figure 9b). The larger influence in the UT/MT of North American pollution than European pollution reflects outflow from convection and the so-called warm conveyor belts (WCBs) originating over the eastern seaboard of North America [*Stohl*, 2001]. In contrast, WCBs rarely originate over Europe [*Stohl*, 2001].

5.4. African Biomass Burning

[30] From late November to early April, about 10–20 ppbv of the UT/MT ozone at Hong Kong is contributed by

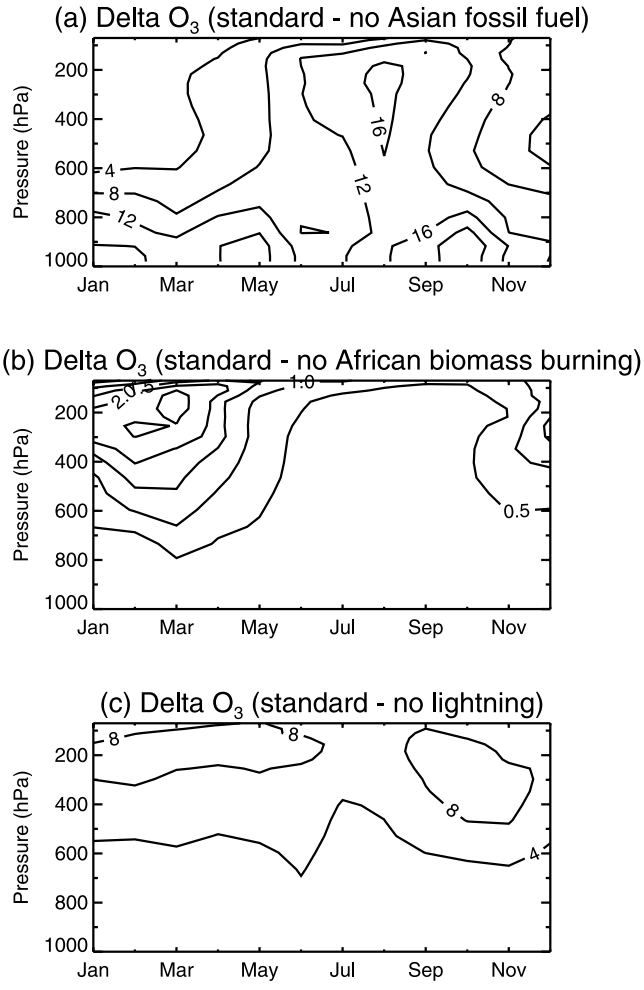

Figure 7. Decreases in ozone concentrations at Hong Kong when (a) Asian fossil fuel emissions, (b) African biomass burning emissions, or (c) lightning NO_x emissions are suppressed, relative to the standard simulation. Values are monthly averages. Contour levels are 4, 8, 12, 16, 20 ppbv for Figures 7a and 7c and 0.5, 1.0, 1.5, 2.0, 3.0 ppbv for Figure 7b.

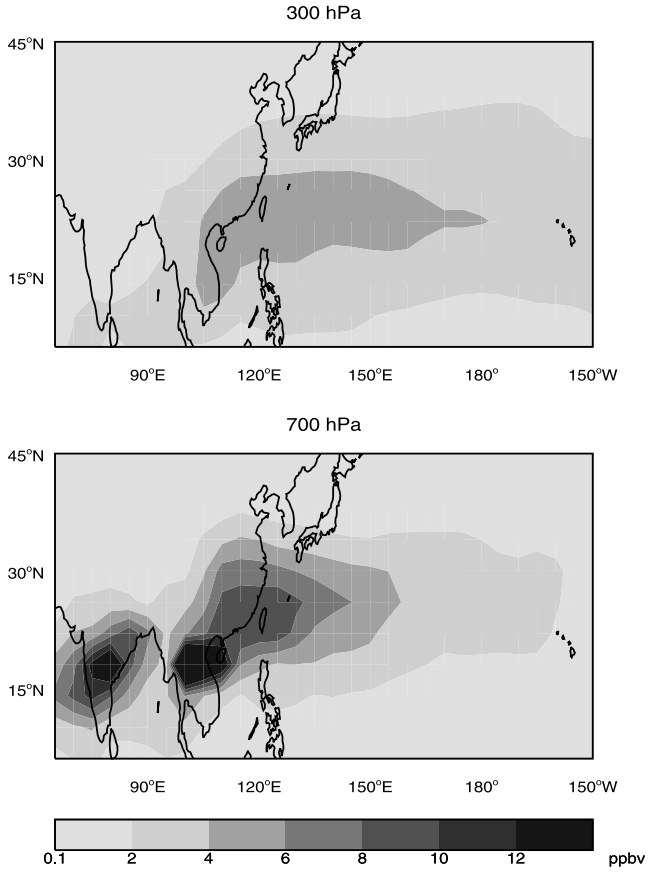

Figure 8. Decreases in ozone concentrations (ppbv) at 300 hPa (upper panel) and 700 hPa (bottom panel) when Southeast Asian biomass burning emissions are suppressed, relative to the standard simulation. Values are monthly averages for March 1996.

the African troposphere (Figure 6b), reflecting intense seasonal biomass burning in sub-Saharan northern Africa [*Marenco et al.*, 1990] as well as lightning [*Martin et al.*, 2002]. Model calculations by *Marufu et al.* [2000] suggest that African biomass burning emissions are responsible for about 35% of the global annual pyrogenic ozone enhancement. Our sensitivity simulation where African biomass burning emissions are suppressed shows a few ppbv decreases in the UT ozone at low-latitude stations (Hong Kong and Naha) from January through March (see Figure 7b for Hong Kong). African air masses convected to the UT merge into the Northern Hemisphere subtropical jet as they travel to the Pacific Rim, leading to a positive correlation between African and stratospheric ozone components in the model on a day-to-day basis.

5.5. Stratospheric Influence

[31] During winter and spring, ozone in the UT at Hong Kong is largely shaped by the alternation between stratospheric influence and intrusion of ozone-poor air from the tropics (Figures 3 and 6c). Stratospheric influence advected from midlatitudes explains the events of high ozone in the UT during January through April; a case study will be discussed in section 6. Stratospheric and tropical influences decrease from April on, reflecting northward shift of the jet stream, the weakening of the Hadley circulation, and the onset of the summer monsoon. At Naha, stratospheric intrusion in the UT has a distinct maximum in spring with frequent events in summer (July–August, not shown). The latter are likely due to stratosphere-troposphere exchange associated with convective complexes [*Poulida et al.*, 1996; *Rood et al.*, 1997], considering that they correlate with anthropogenic pollution from Asia in the model. Stratospheric contribution to UT ozone is maximum in winter for the higher-latitude Japanese stations, consistent with current knowledge of stratosphere-troposphere exchange [*Austin and Midgley*, 1994].

5.6. Lightning

[32] Lightning influence, as indicated with a sensitivity simulation where NO_x emissions from lightning are shut off, is shown in Figure 7c for Hong Kong and in Figure 10 for the globe at 300 hPa. Lightning has the strongest influence over subsiding regions which receive the accumulated effect of ozone production in the UT [*Jacob et al.*, 1996; *Martin et al.*, 2002]. The decrease in ozone concentrations is up to ~8 ppbv in the UT/MT over Hong Kong and Naha, with a summertime minimum. Much less influence is seen at the higher-latitude Japanese stations; the meridional gradient of influence is particularly strong in winter and spring. The summer minimum at low latitudes is somewhat surprising if one considers that deep convection over the Asian continent is maximum at this time of the year. It reflects the westward UT transport of lightning outflow away from the Pacific Rim, as discussed in section 4. Instead, lightning outflow from the Indian subcontinent and Southeast Asia makes a major contribution to summertime tropospheric ozone over the Middle East [*Li et al.*, 2001].

6. Case Studies

[33] We present here some case studies from Hong Kong and other ozonesonde records to illustrate some of the major features of the ozone observations along the Pacific Rim, including alternation between low and high ozone in the wintertime UT, springtime ozone layer enhancements, and high ozone episodes in summer and fall.

6.1. Alternation Between Low and High Ozone in the Wintertime UT

[34] As noted above, a remarkable feature of the observations at Hong Kong is the alternation between low and high ozone in the wintertime UT (Figure 3). This feature is reproducible from year to year (September 1995 to April 1997). Back trajectories and our model results relate the low ozone to intrusions of tropical air and the high ozone to intrusions of midlatitude stratospherically-influenced air. Intrusions of tropical air are favored in winter when the Hadley circulation is at its seasonal maximum intensity [*Ding*, 1994]. We illustrate this point here with a case study for December 24, 1996 and January 6, 1997 (Figure 11).

[35] On December 24, the air flow in the UT over South China is from the tropics and carries low ozone upwelled in the ascending branch of the East Asia local Hadley circulation (Figure 11, middle left panel). By January 6, 1997, this circulation has shifted to the east and the UT flow over

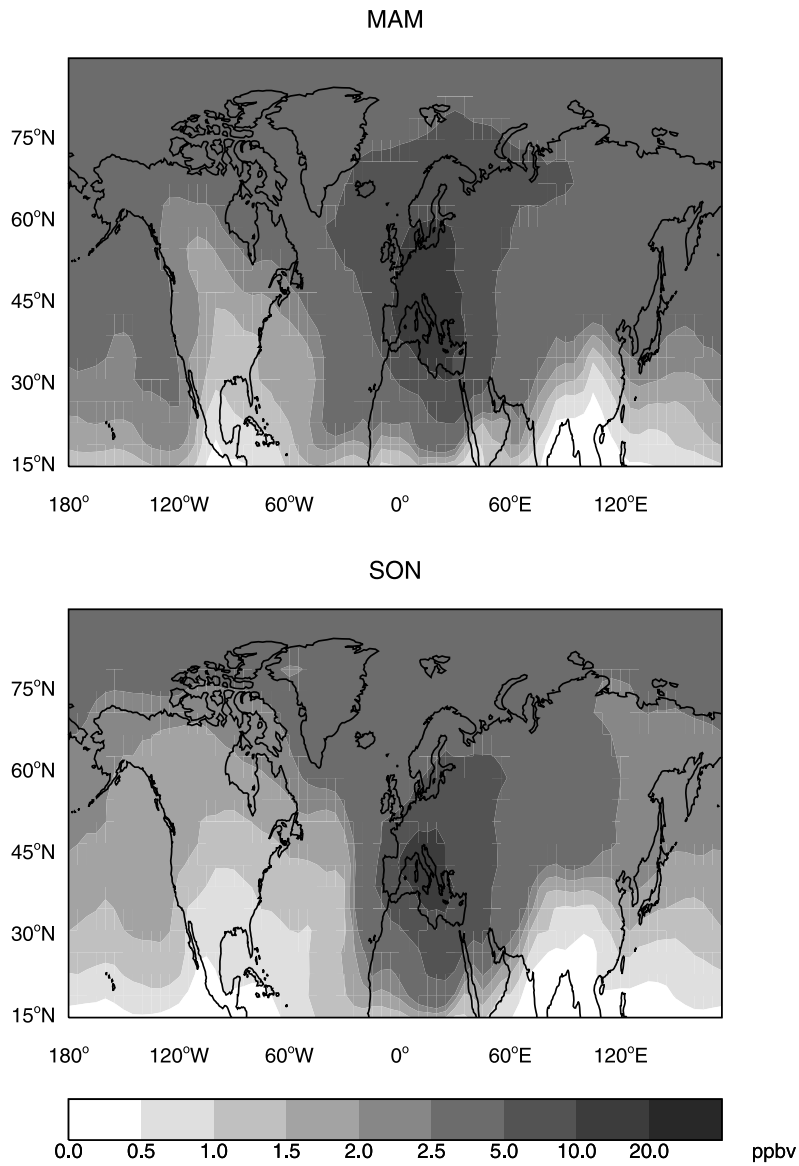

Figure 9. Decreases in ozone concentrations (ppbv) (a) at 900 hPa when European fossil fuel emissions are suppressed, (b) at 300 hPa when North American fossil fuel emissions are suppressed, relative to the standard simulation. Values are averages for spring (March–April–May) and fall (September–October–November) 1996. See color version of this figure at back of this issue.

Hong Kong is instead from the northwest (Figure 11, middle right panel); the intensification and southward movement of westerlies (subtropical jet stream) leads to the intrusion of stratospheric ozone into the tropical troposphere (Figure 11, bottom right panel).

[36] Ozone minima in the UT over Hong Kong associated with tropical convective outflow (30–40 ppbv) are never as low as values found in tropical convective outflow over other regions (<20 ppbv) including the western Pacific Ocean [e.g., *Kley et al.*, 1996; *Browell et al.*, 1996; *Newell et al.*, 1997], the Indian Ocean [*de Laat et al.*, 1999], or the eastern U.S. and North Atlantic Ocean [*Grant et al.*, 2000]. We find in the model that such low values do not occur over Hong Kong because of ozone production from Asian pollution and lightning emissions affecting the tropical convective outflow, as discussed in section 4.

6.2. Springtime Ozone Layer Enhancements

[37] Asian biomass burning outflow to the Pacific in spring peaks in the lower free troposphere [*Liu et al.*, 1999; *Bey et al.*, 2001b], but high springtime ozone events over Hong Kong are also observed in the UT. Figures 12a–12e shows daily ozonesonde profiles during the period of April 11–15, 1996, illustrating some of these events, associated with moderately high humidity (20–30%). The corresponding back trajectories all pass over continental Southeast Asia, suggesting a biomass burning origin similar to that in the LT. The model usually underestimates or

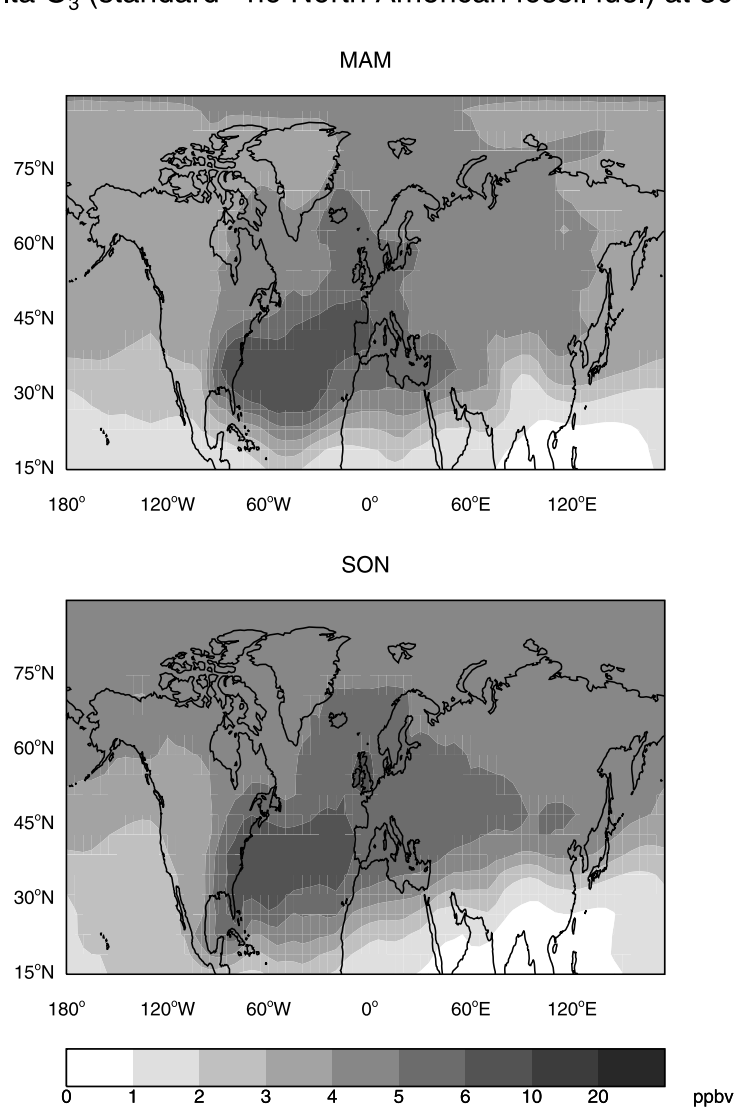

Figure 9. (continued)

misses these ozone layer enhancements in both the UT and the LT, but does show enhanced CO of Asian biomass burning origin (Figure 12). High values of biomass burning CO and to a lesser extent Asian fossil fuel CO concentrations indicate the important role of deep convection over Indochina in lifting biomass burning and anthropogenic pollution from the surface to the UT. Sensitivity simulations show comparable contributions to the UT ozone from biomass burning, Asian fossil fuel, and lightning emissions.

[38] The limited ability of the model to simulate the ozone layer enhancements in both the LT and the UT could be due to the following factors among others. Since the layers of enhanced ozone in the LT generally have their bases at about 2 km with a thickness of about 2–3 km, weak vertical transport and mixing would be adequate to lift ozone and its precursors up from the boundary layer to lower free troposphere. The fire buoyancy not accounted for in the model is believed to contribute to the ventilation of biomass burning pollution and thus to the formation of ozone layer enhancements over Hong Kong. Also, many biomass burning activities over continental Southeast Asia take place in mountainous forest regions [*Stott*, 1988; *Jones*, 1997] where isoprene and other hydrocarbon emissions may lead to efficient production of ozone [*Pickering et al.*, 1992]. Satellite observations have shown unusually active biomass burning (relative to climatology) over this area in the spring of 1996 (R. Martin, personal communication, 2001), in particular in the northern part of the Indochina where high terrain elevations facilitate the impact of biomass burning emissions on downwind regions (H. Liu et al., manuscript in preparation, 2002). The issue in discussion is further complicated by the episodic nature of biomass burning activities.

[39] Events of Asian biomass burning influence can also be seen midway across the Pacific at Hilo. Ozonesonde observations on April 3, 1996 at Hilo show a pronounced ozone peak (~80 ppbv) in the MT (~500 hPa) (Figure 12f). The model captures this peak with the right magnitude, although it does not capture the overlying minimum.

6.3. Ozone Episodes in Summer

[40] Even though tropospheric ozone at the lower-latitude Pacific Rim stations is at its seasonal minimum in summer,

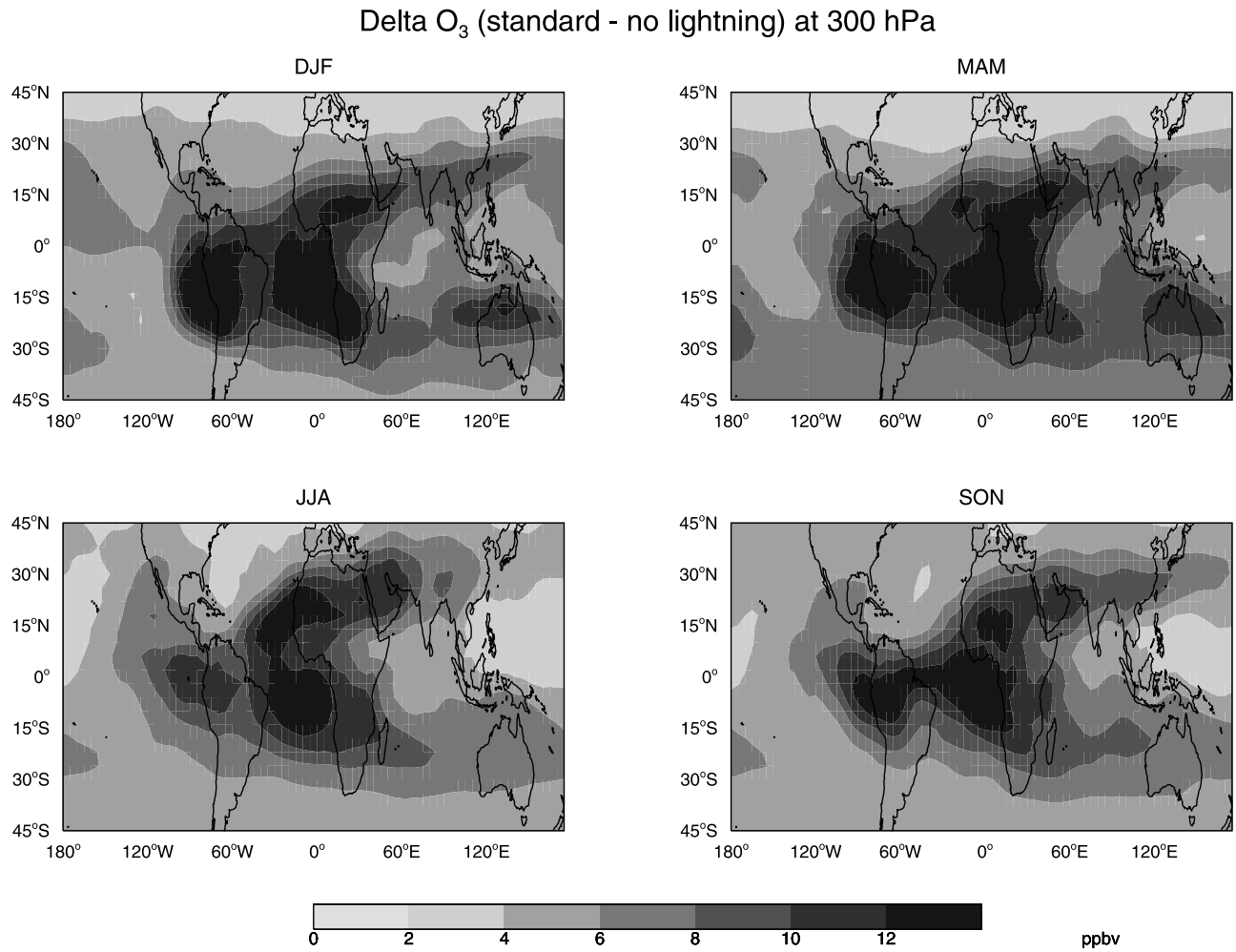

Figure 10. Decreases in ozone concentrations (ppbv) at 300 hPa when lightning NO_x emissions are suppressed, relative to the standard simulation for 1996. Values are seasonal averages for 1996. See color version of this figure at back of this issue.

ozone enhancements are occasionally observed in the free troposphere. Here we examine such an episode on August 6, 1996 (Figure 3). This episode reflects an interruption of the monsoon by a tropical cyclone. On August 6, 1996, ozonesonde observations at Hong Kong show a broad maximum of mixing ratio (~75–110 ppbv) in the MT, with lower ozone in the LT and UT (Figure 13). Kagoshima on the same day also shows a peak of ozone mixing ratio (~70 ppbv) at ~400 hPa. Back trajectories indicate that the mid-tropospheric air mass remained over the East China Sea for a few days before it was advected southward to Hong Kong. During July 31–August 2, the tropical cyclone Herb made a landfall in East China and subsequently evolved into a continental low pressure system [*Hong Kong Observatory* (*HKO*), 1996], which may have caused widespread lifting of ozone and/or its precursors from the boundary layer into the MT and UT. The explicit transport mechanism for this pollution is however complicated. The standard simulation with $4^\circ \times 5^\circ$ resolution does not capture the MT ozone layer at Hong Kong, but a simulation with $2^\circ \times 2.5^\circ$ resolution significantly improves the result (Figure 13). In this layer is enhanced Asian fossil fuel CO, and sensitivity simulations indicate that without Asian fossil fuel emissions there would be no ozone enhancement. The model reproduces the MT ozone enhancement concurrently observed at Kagoshima with overestimates below and above.

[41] High ozone due to anthropogenic pollution is observed frequently in the UT over Hong Kong in summer, in which case trajectories are usually very similar; pollution along the eastern Asian coast is lifted into the UT by deep convection followed by northerly transport as part of the Tibetan anticyclone (Figure 5c). One such case is August 21, 1996, when observed ozone shows high values in the UT (Figure 14). The model reproduces well the strong vertical gradient of ozone and the sensitivity simulation indicates maximum influence in the UT from Asian anthropogenic emissions.

6.4. Ozone Episodes Over Hong Kong in Fall

[42] Our model sensitivity calculations indicate that, at lower latitudes (Hong Kong and Naha), Asian pollution influence on ozone is larger in fall than in spring, not only in the boundary layer but in the free troposphere; the latter is also somewhat true for lightning influence (Figure 7). Indeed, observations at Hong Kong in October–November 1996 show high ozone events (60–90 ppbv) in the MT-UT (Figure 3). Here we present a case study for October 9, 1996. Observations at Hong Kong on that day show sub-

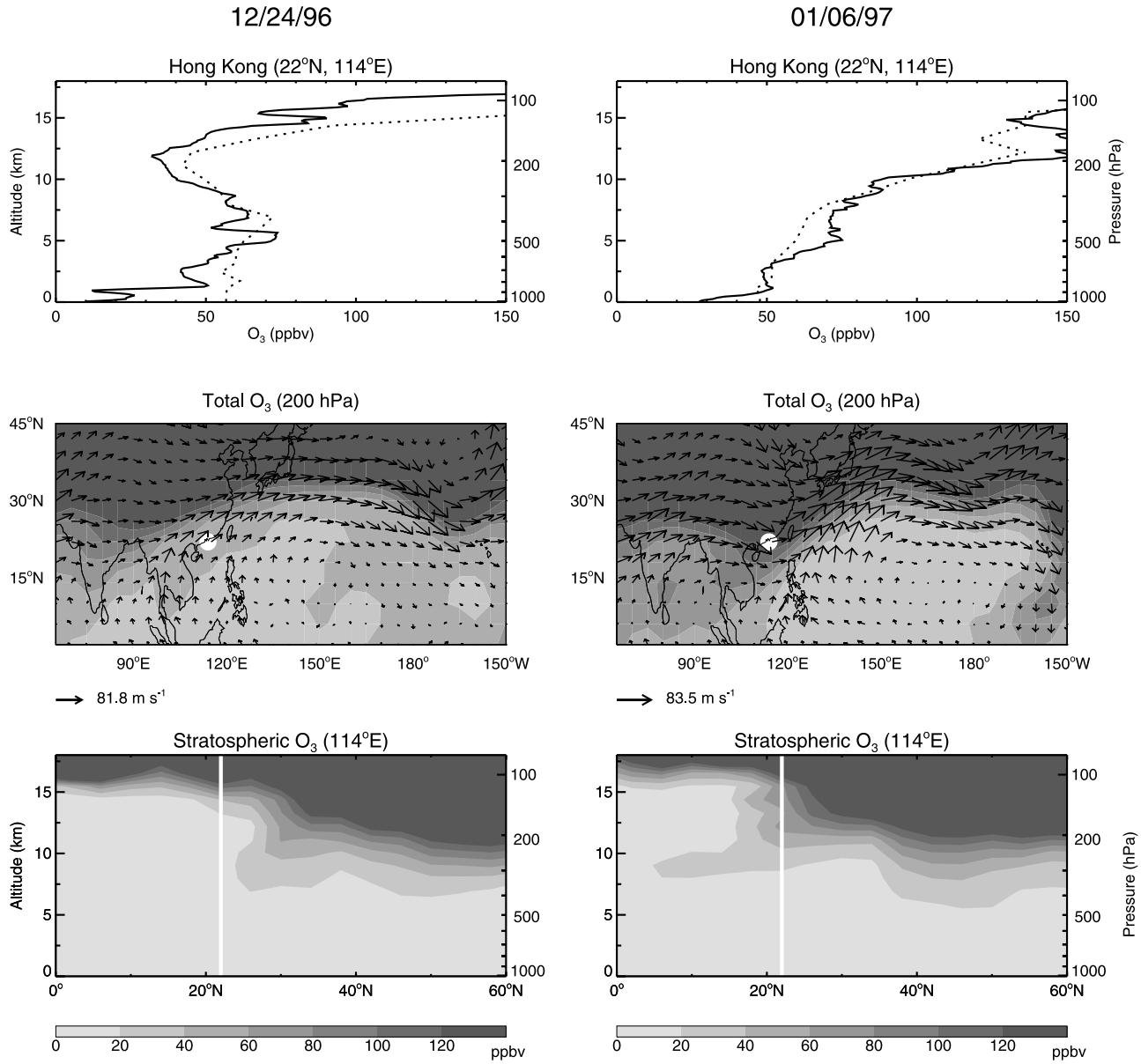

Figure 11. Case study illustrating the alternation between low and high ozone in the wintertime upper troposphere over Hong Kong. The top panels show ozonesonde profiles on December 24, 1996 and January 6, 1997. Observations (solid lines) are compared to model results for the corresponding days (dotted lines). The middle and bottom panels show additional model results for those days: (1) ozone concentrations and wind vectors at 200 hPa; (2) latitude-altitude cross-section at the longitude of Hong Kong (114°E) for the tagged ozone tracer originating in the stratosphere. The white dots and vertical lines correspond to the location of Hong Kong. See color version of this figure at back of this issue.

stantial enhancements of ozone in much of the troposphere (600–150 hPa) and model sensitivity calculations indicate large influences from both Asian fossil fuel and lightning emissions (Figure 15). We find that this event is driven by lifting ahead of a cold front sweeping across China [*HKO*, 1996].

[43] Cold fronts have been recognized previously as a major pathway for outflow of Asian pollution to the Pacific [*Liu et al.*, 1997; *Carmichael et al.*, 1998; *Yienger et al.*, 2000; *Bey et al.*, 2001b]. In spring, these fronts are very frequent [*Chen et al.*, 1991; *Zhang et al.*, 1997] but are then usually too far north to influence Hong Kong, where low-latitude air prevails (Figure 5a). In the fall, by contrast, the northeasterly monsoon sweeps the Asian pollution toward Hong Kong. This pollution is exported to the Pacific by cold fronts and convection. Subsequent active photochemistry leads to strong Asian pollution influence throughout the troposphere at low latitudes.

7. Contributions to Asian Outflow of Ozone to the Pacific

[44] We discuss briefly in this section for different seasons of 1996 the relative contributions from different

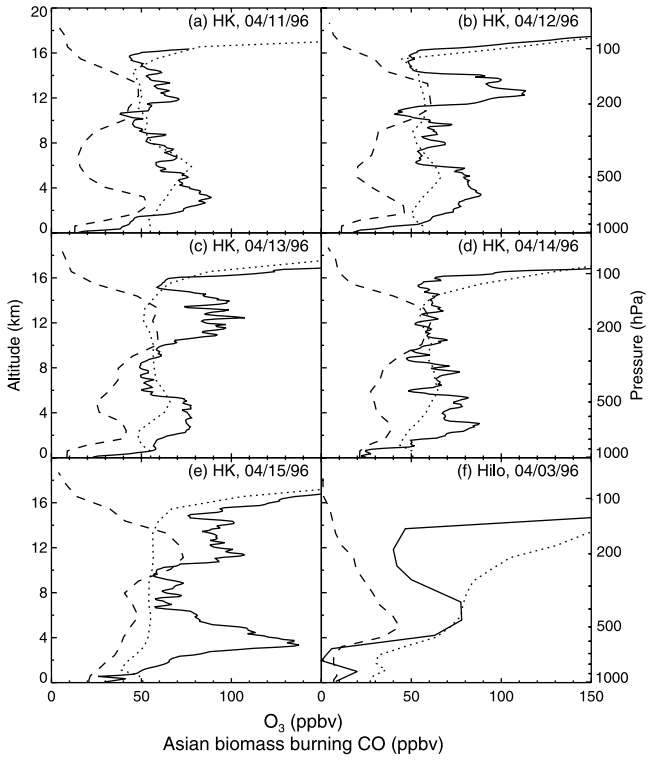

Figure 12. Ozonesonde profiles at (a)–(e) Hong Kong on April 11–15, 1996, and (f) Hilo on April 3, 1996. Observations (solid lines) are compared to model results for the corresponding days (dotted lines). Also shown are Asian biomass burning CO concentrations (dashed line) from a tagged tracer simulation.

sources to the Asian outflow of ozone to the Pacific. The relative contribution from a given source is determined by difference from the standard simulation in a sensitivity simulation where that source is suppressed. Figure 16 shows the relative contributions to the eastward flux of ozone integrated for the 1000–200hPa column through a wall at 150°E between 10 and 60°N, from Asian fossil fuel, European fossil fuel, North American fossil fuel, Asian biomass burning, lightning, and African biomass burning emissions. Also shown in Figure 16 (dashed line) is the total eastward flux of ozone (scaled down by a factor of 20) in the standard simulation.

[45] Anthropogenic Asian influence on the Asian outflow flux of ozone to the Pacific is maximum in spring and fall, and is minimum in winter and summer. The low value in winter reflects weak photochemical activity. The low value in summer reflects the prevailing easterly flow away from the Pacific (section 4). The contribution from Asian biomass burning is maximum in spring and insignificant in other seasons. African biomass burning influence is maximum in early spring. European anthropogenic influence peaks in spring. By contrast, the maximum influence of North American pollution is in late fall. Lightning influence also peaks in late fall.

[46] Throughout the year we find that anthropogenic sources in Asia make the largest single contribution to the Asian outflow flux of ozone over the Pacific (Figure 16). Second is lightning, due to strong sources over both South Asia and Africa. Remarkably, North American anthropogenic sources contribute more to the Asian outflow flux of ozone than European anthropogenic sources, reflecting efficient uplifting by the warm conveyor belts and by convection over and downwind off the eastern United States (section 5).

8. Summary and Conclusions

[47] We have used a global 3-D model of tropospheric chemistry driven by assimilated meteorological data to analyze ozonesonde observations along the Asian Pacific Rim. Our aim was to understand the contributions from different sources to the tropospheric ozone budget in that region for different seasons and altitudes. We analyzed ozonesonde observations at four stations (Hong Kong, Naha, Kagoshima, and Sapporo) extending from 22°N to 43°N along the Pacific Rim, and one (Hilo) over the remote Pacific, with a particular focus on the year of 1996 at Hong Kong where an extensive data set is available.

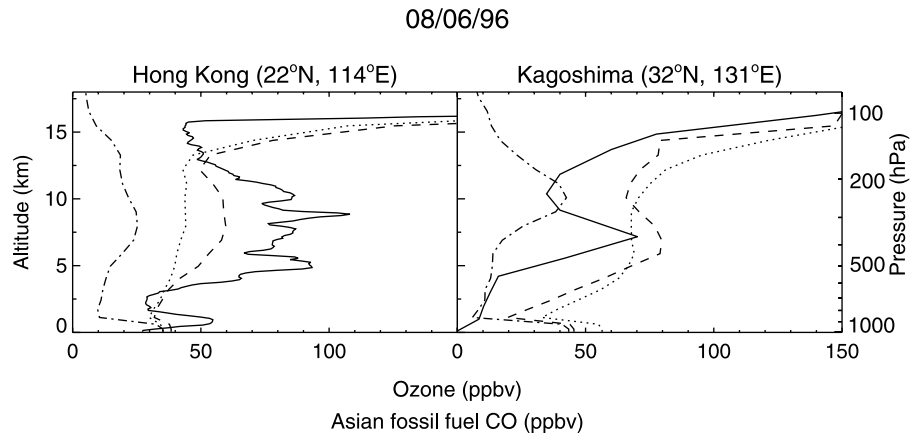

Figure 13. Summertime ozone pollution event in the middle troposphere over Hong Kong and Kagoshima on August 6, 1996. The solid lines show ozonesonde observations, and the dotted lines show model results. Also shown are ozone concentrations simulated with 2° × 2.5° model resolution (dashed line) and Asian fossil fuel CO concentrations (dash-dotted line).

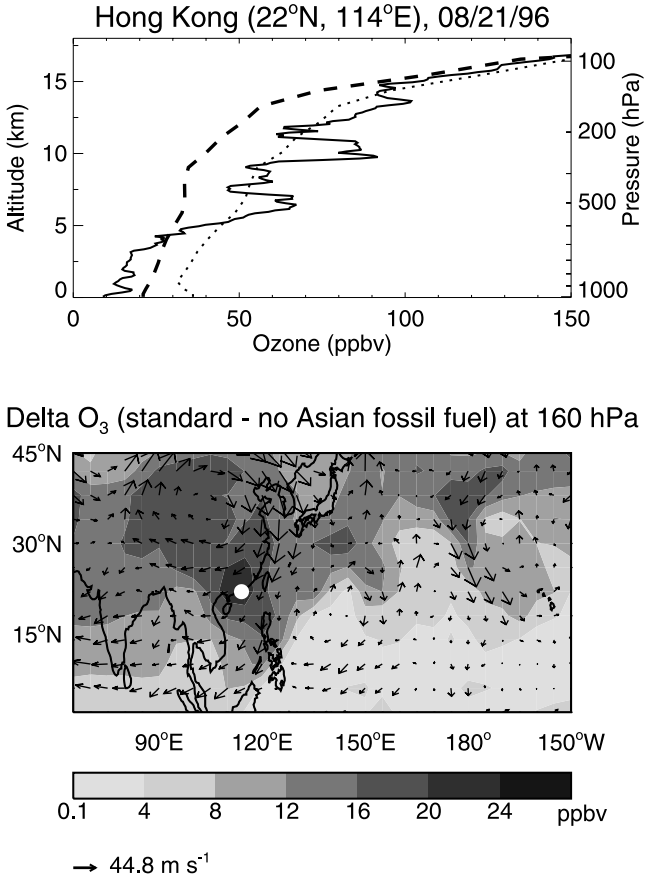

Figure 14. Summertime ozone pollution event in the upper troposphere over Hong Kong on August 21, 1996. The solid line shows ozonesonde observations, and the dotted line shows model results. Also shown as a vertical profile are simulated ozone concentrations when Asian fossil fuel emissions are suppressed (dashed line). The map shows decreases in ozone concentrations (ppbv) at 160 hPa (13 km), when Asian fossil fuel emissions are shut off, relative to the standard simulation. Arrows are wind vectors, and the white dot shows the location of Hong Kong. See color version of this figure at back of this issue.

[48] The seasonal cycle of ozone has a spring maximum and summer minimum at low latitudes (Hong Kong and Naha), but shifts to a summer maximum in the middle and upper troposphere (MT-UT) at higher latitudes (Kagoshima and Sapporo). The springtime lower troposphere (LT) maximum is due primarily to Southeast Asian biomass burning, and the springtime UT maximum reflects the phase overlap of ozone transported from the stratosphere and ozone produced in the troposphere [*Wang et al.*, 1998]. The shift to a summer maximum at higher latitudes is due to seasonal photochemical production in the MT-UT.

[49] We investigated the sources of tropospheric ozone along the Asian Pacific Rim by tagging ozone produced from different source regions and by model sensitivity calculations. We found that Asian sources dominate the ozone budget throughout the troposphere, except for the winter- spring UT/MT where stratospheric and other sources are important. Maximum Asian pollution influence in the LT occurs in spring and fall at lower latitudes, and in late spring and summer at higher latitudes; maximum influence in the MT-UT is in summer when rapid convective transport of ozone precursors from the continental boundary layer leads to unusually strong photochemical production of ozone (6–10 ppbv/day). Maximum European pollution influence along the Pacific Rim takes place in the LT (<4

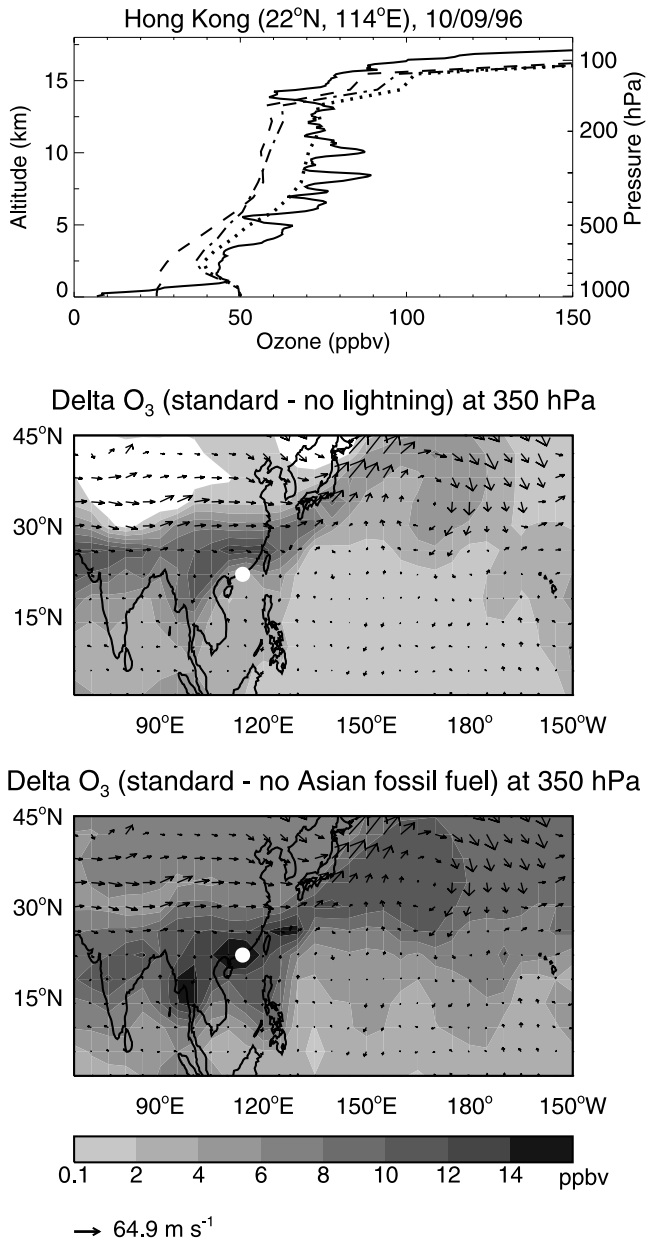

Figure 15. High-ozone episode over Hong Kong in fall (October 9, 1996). The solid line shows ozonesonde observations, and the dotted line shows model results (upper panel). Also shown as vertical profiles are ozone concentrations when lightning NO_x emissions (dash-dotted line) or Asian fossil fuel emissions (dashed line) are suppressed. Maps show decreases in ozone (ppbv) at 350 hPa (8 km) when lightning emissions (middle panel) or Asian fossil fuel emissions (bottom panel) are suppressed, relative to the standard simulation. Arrows are wind vectors, and the white dots show the location of Hong Kong. See color version of this figure at back of this issue.

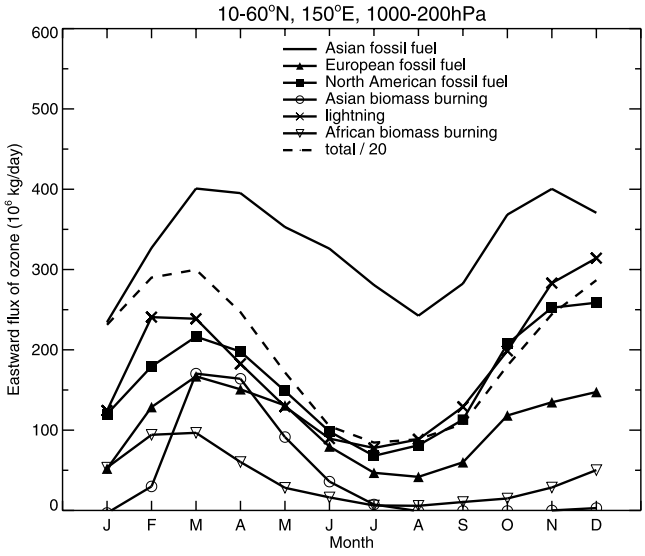

Figure 16. Relative contributions from different sources to the Asian outflow flux of ozone over the Pacific as a function of season in 1996. The Asian outflow flux is defined as the eastward flux (10^6 kg/day) integrated for the 1000–200hPa column through a wall located at 150°E between 10 and 60°N. Contributions from individual sources (i.e., Asian fossil fuel, European fossil fuel, North American fossil fuel, Asian biomass burning, lightning, African biomass burning) are determined by subtraction from the standard simulation in a sensitivity simulation where the source is suppressed. The total Asian outflow flux of ozone in the standard simulation (scaled down by a factor of 20) is plotted as a dashed line. All values are monthly averages.

km) in spring, but with an ozone enhancement of less than 5 ppbv. North American pollution influence is maximum in the UT in fall and exceeds European pollution influence in the UT/MT, reflecting more efficient uplift by convection and by the warm conveyor belts at the eastern seaboard of North America. African biomass burning and lightning emissions make major contributions to the Pacific Rim observations in the MT-UT at lower latitudes. Stratospheric influence is responsible for major events of high ozone in the UT and is important in the MT during winter/spring. In particular, stratospheric influence at low latitudes is determined by southern shifts of the subtropical jet and can extend into the deep tropics. Lightning influence is important in the UT/MT at low latitudes, with a summer minimum due to westward transport of lightning outflow around the Tibetan anticyclone and away from the Pacific Rim.

[50] We conducted case studies to further examine the sources of high/low ozone in different seasons. In winter/spring, the UT ozone at lower latitudes is largely shaped by the alternation between intrusion of tropical air (low ozone) and stratospheric influence (high ozone). The former is most favorable in winter when the East Asia local Hadley circulation reaches its seasonal maximum intensity [*Ding*, 1994]. The shift from the former to the latter appears to be accompanied by eastward shift of the Hadley cell, allowing stratospherically influenced air from northern midlatitudes to flow over the Pacific Rim. Even under conditions of tropical convective outflow, ozone concentrations in the UT are still relatively high due to contributions from Asian pollution and lightning emissions.

[51] Biomass burning in Southeast Asia in spring leads to substantial enhancements of tropospheric ozone at all altitudes over the Pacific Rim (<32°N) and evidence of this enhancement extends across the Pacific to the ozonesonde observations over Hilo. Along the Pacific Rim this seasonal biomass burning influence is strongest in the lower free troposphere, but deep convection also produces biomass burning enhancements of ozone in the UT/MT which are seen over Hong Kong and Hilo.

[52] In summer, tropospheric ozone is at its seasonal minimum at the lower latitudes of the Pacific Rim. The monsoon lifts Asian pollution to the UT where much of it gets caught in the westward circulation around the Tibetan anticyclone, away from the Pacific. Mid-level convection and stagnation occasionally produce elevated ozone layers in the MT, and two such episodes observed at Hong Kong were analyzed.

[53] In fall, the South China coast region is a photochemically active region as the building continental high leads to clear skies and southward transport of pollution. Frontal and convective lifting of this pollution produces elevated ozone layers in the free troposphere over Hong Kong. Frontal lifting of pollution is more frequent in fall than in spring at the lower latitudes of the Pacific Rim, in contrast to higher latitudes where frontal lifting is most efficient in spring.

[54] We investigated the relative contributions from different sources to the Asian outflow flux of ozone over the Pacific. This flux is maximum in spring and fall, and includes a major contribution year-round from anthropogenic sources in Asia as well as from lightning. Anthropogenic sources in North America make a bigger contribution to the Asian outflow than anthropogenic sources in Europe, reflecting more efficient uplift by convection and frontal activity. African biomass burning contributes to Asian outflow from December through April while Asian biomass burning influence is concentrated in March–April.

[55] We find overall that tropospheric ozonesonde observations along the Pacific Rim are consistent with current understanding of tropospheric chemistry as quantified by the GEOS-CHEM global 3-D model. While this result encourages the use of such models to analyze Asian outflow and long-term trends of ozone, our ability to further constrain the model is still limited by available measurements and current understanding of physical and chemical processes in the atmosphere. Improved understanding is needed with respect to variability in meteorology in this region, stratosphere-troposphere exchange, biomass burning and lightning activities, as well as intercontinental transport. Projected increases in anthropogenic emissions of ozone precursors in Asia [*van Aardenne et al.*, 1999] are expected to lead to a positive trend of tropospheric ozone in the region, and detection and interpretation of this trend will be complicated by the above factors in particular variability in biomass burning and lightning. With increasing satellite observations becoming available in the future, constraints on these sources are expected to be greatly improved. Several years of coordinated and intensive year-round measurements at the established ozonesonde stations along

the Asian Pacific Rim should be quite helpful in better constraining the model. Studies of orographic influence on pollution transport should also be encouraged.

[56] **Acknowledgments.** We would like to thank Jennifer Logan and Ken Pickering for helpful discussions and comments. This research was funded by the NASA Atmospheric Chemistry Modeling and Analysis Program (ACMAP), by the Hong Kong Polytechnic University, and by the Research Grants Council of Hong Kong. We acknowledge the help given by Wen Lam Chang and the Hong Kong Observatory's personnel at King's Park meteorological station in the launching of ozonesondes. We also acknowledge the contribution to the GEOS-CHEM model development by B. D. Field, A. M. Fiore, Q. Li, J. A. Logan, A. C. Staudt, and R. M. Yevich.

References

Akimoto, H., H. Nakane, and Y. Matsumoto, The chemistry of oxidant generation: Tropospheric ozone increase in Japan, in *Chemistry of the Atmosphere: The Impact on Global Change*, edited by J. Calvert, pp. 261–273, Blackwell Sci., Malden, Mass., 1994.

Allen, D. J., R. B. Rood, A. M. Thompson, and R. D. Hudson, Three-dimensional radon 222 calculations using assimilated meteorological data and a convective mixing algorithm, *J. Geophys. Res.*, *101*, 6871–6881, 1996.

Austin, J. F., and R. P. Midgley, The climatology of the jet stream and stratospheric intrusions of ozone over Japan, *Atmos. Environ.*, *28*, 39–52, 1994.

Bell, N., L. Hsu, D. J. Jacob, M. G. Schultz, D. R. Blake, J. H. Butler, D. B. King, J. M. Lobert, and E. Maier-Reimer, Methyl iodide: Atmospheric budget and use as a tracer of marine convection in global models, *J. Geophys. Res.*, *107*(D17), 4340, doi:10.1029/2001JD001151, 2002.

Berntsen, T., I. S. A. Isaksen, W. C. Wang, and X. Z. Liang, Impacts of increased anthropogenic emissions in Asia on tropospheric ozone and climate: A global 3-D model study, *Tellus, Ser. B*, *48*, 13–32, 1996.

Bey, I., D. J. Jacob, R. M. Yantosca, J. A. Logan, B. Field, A. M. Fiore, Q. Li, H. Liu, L. J. Mickley, and M. Schultz, Global modeling of tropospheric chemistry with assimilated meteorology: Model description and evaluation, *J. Geophys. Res.*, *106*, 23,073–23,096, 2001a.

Bey, I., D. J. Jacob, J. A. Logan, and R. M. Yantosca, Asian chemical outflow to the Pacific: Origins, pathways and budgets, *J. Geophys. Res.*, *106*, 23,097–23,114, 2001b.

Blake, N. J., et al., Large scale latitudinal and vertical distributions of NMHCs and selected halocarbons in the troposphere over the Pacific Ocean during the March–April 1999 Pacific Exploratory Expedition (PEM-Tropics B), *J. Geophys. Res.*, *106*, 32,627–32,644, 2001.

Browell, E. V., et al., Large-scale air mass characteristics observed over western Pacific during summertime, *J. Geophys. Res.*, *101*, 1691–1712, 1996.

Carmichael, G. R., I. Uno, M. J. Phadnis, Y. Zhang, and Y. Sunwoo, Tropospheric ozone production and transport in the springtime in east Asia, *J. Geophys. Res.*, *103*, 10,649–10,671, 1998.

Chameides, W. L., et al., Is ozone pollution affecting crop yields in China?, *Geophys. Res. Lett.*, *26*, 867–870, 1999.

Chan, C. Y., L. Y. Chan, Y. G. Zheng, J. M. Harris, S. J. Oltmans, and S. Christopher, Effect of 1997 Indonesian forest fires on tropospheric ozone enhancement, radiative forcing, and temperature change over the Hong Kong region, *J. Geophys. Res.*, *106*, 14,875–14,885, 2001.

Chan, L. Y., H. Y. Liu, K. S. Lam, T. Wang, S. J. Oltmans, and J. M. Harris, Analysis of the seasonal behavior of tropospheric ozone at Hong Kong, *Atmos. Environ.*, *32*, 159–168, 1998.

Chan, L. Y., C. Y. Chan, H. Y. Liu, S. Christopher, S. J. Oltmans, and J. M. Harris, A case study on the biomass burning in Southeast Asia and enhancement of tropospheric ozone over Hong Kong, *Geophys. Res. Lett.*, *27*, 1479–1482, 2000.

Chandra, S., J. R. Ziemke, P. K. Bhartia, and R. V. Martin, Tropical tropospheric ozone: Implications for biomass burning, *J. Geophys. Res.*, *107*(D14), 4188, doi:10.1029/2001JD000447, 2002.

Chen, S., Y. Kuo, P. Zhang, and Q. Bai, Synoptic climatology of cyclogenesis over East Asia, 1958–1987, *Mon. Weather Rev.*, *11*, 1407–1418, 1991.

Crutzen, P. J., Tropospheric ozone: An overview, in *Tropospheric Ozone*, edited by I. S. A. Isaksen, pp. 3–32, D. Reidel, Norwell, Mass., 1988.

de Laat, A. T. J., M. Zachariasse, G. J. Roelofs, P. vanVelthoven, R. R. Dickerson, K. P. Rhoads, S. J. Oltmans, and J. Lelieveld, Tropospheric O_3 distribution over the Indian Ocean during spring 1995 evaluated with a chemistry-climate model, *J. Geophys. Res.*, *104*, 13,881–13,893, 1999.

Ding, Y. H., *Monsoons Over China*, Kluwer Acad., Norwell, Mass., 1994.

Duncan, B. N., R. V. Martin, A. Staudt, R. Yevich, and J. A. Logan, Interannual and seasonal variability of biomass burning emissions constrained by satellite observations, *J. Geophys. Res.*, *107*, doi:10.1029/2002JD002378, in press, 2002.

Fiore, A. M., D. J. Jacob, I. Bey, R. M. Yantosca, B. D. Field, A. C. Fusco, and J. G. Wilkinson, Background ozone over the United States in summer: Origin, trend, and contribution to pollution episodes, *J. Geophys. Res.*, *107*(D15), 4275, doi:10.1029/2001JD000982, 2002.

Grant, W. B., et al., A case study of transport of tropical marine boundary layer and lower tropospheric air masses to the northern midlatitude upper troposphere, *J. Geophys. Res.*, *105*, 3757–3769, 2000.

Halpert, M. S., and G. D. Bell, Climate assessment for 1996, *Bull. Am. Meteorol. Soc.*, *78*, 1–49, 1997.

Harris, J. M., and J. D. W. Kahl, Analysis of 10-day isentropic flow patterns for Barrow, Alaska: 1985–1992, *J. Geophys. Res.*, *99*, 25,845–25,855, 1994.

Hong Kong Observatory (HKO), Monthly weather summary, Hong Kong, 1996.

Jacob, D. J., et al., Origin of ozone and NO_x in the tropical troposphere: A photochemical analysis of aircraft observations over the South Atlantic Basin, *J. Geophys. Res.*, *101*, 24,235–24,350, 1996.

Jacob, D. J., J. A. Logan, and P. P. Murti, Effect of rising Asian emissions on surface ozone in the United States, *Geophys. Res. Lett.*, *26*, 2175–2178, 1999.

Jacobson, M. Z., and R. P. Turco, A sparse-matrix, vectorized GEAR code for atmospheric transport models, *Atmos. Environ.*, *33*, 273–284, 1994.

Jones, S. H., The distribution of vegetation fire in mainland Southeast Asia: Spatio-temporal analysis of AVHRR 1km data for the 1992/93 dry season, *Rep. EUR 17282 EN*, 48 pp., Eur. Comm., Brussels, 1997.

Jonson, J. E., J. K. Sunder, and L. Tarrason, Model calculations of present and future levels of ozone and ozone precursors with a global and a regional model, *Atmos. Environ.*, *35*, 525–537, 2001.

Kentarchos, A. S., G. J. Roelofs, and J. Lelieveld, Altitude distribution of tropospheric ozone over the northern Hemisphere during 1996, simulated with a chemistry-general circulation model at two different horizontal resolutions, *J. Geophys. Res.*, *106*, 17,453–17,469, 2001.

Kley, D., P. J. Crutzen, H. G. J. Smit, H. VÖmel, S. J. Oltmans, H. Grassl, and V. Ramanathan, Observations of near-zero ozone concentrations over the convective Pacific: Effects on air chemistry, *Science*, *274*, 230–233, 1996.

Lacis, A. A., D. J. Wuebbles, and J. A. Logan, Radiative forcing of climate by changes in the vertical distribution of ozone, *J. Geophys. Res.*, *95*, 9971–9981, 1990.

Lam, K. S., T. J. Wang, L. Y. Chan, T. Wang, and J. Harris, Flow patterns influencing the seasonal behavior of surface ozone and carbon monoxide at a coastal site near Hong Kong, *Atmos. Environ.*, *35*, 3121–3135, 2001.

Lee, S., H. Akimoto, H. Nakane, S. Kurnosenko, and Y. Kinjo, Lower tropospheric ozone trend observed in 1989–1997 at Okinawa, Japan, *Geophys. Res. Lett.*, *25*, 1637–1640, 1998.

Lelieveld, J., and F. J. Dentener, What controls tropospheric ozone?, *J. Geophys. Res.*, *105*, 3531–3551, 2000.

Li, Q., et al., A tropospheric ozone maximum over the Middle East, *Geophys. Res. Lett.*, *28*, 3235–3238, 2001.

Li, Q., et al., Transatlantic transport of pollution and its effects on surface ozone in Europe and North America, *J. Geophys. Res.*, *107*(D13), 4166, doi:10.1029/2001JD001422, 2002.

Lin, S.-J., and R. B. Rood, Multidimensional flux-form semi-Lagrangian transport schemes, *Mon. Weather Rev.*, *124*, 2046–2070, 1996.

Liu, C. M., M. Buhr, and J. T. Merill, Ground-based observations of ozone, carbon monoxide, and sulfur dioxide at Kenting, Taiwan, during the PEM West B campaign, *J. Geophys. Res.*, *102*, 28,613–28,625, 1997.

Liu, H. Y., W. L. Chang, S. J. Oltmans, L. Y. Chan, and J. M. Harris, On springtime high ozone events in the lower troposphere from Southeast Asian biomass burning, *Atmos. Environ.*, *33*, 2403–2410, 1999.

Liu, H. Y., D. J. Jacob, I. Bey, and R. M. Yantosca, Constraints from ^{210}Pb and ^{7}Be on wet deposition and transport in a global three-dimensional chemical tracer model driven by assimilated meteorological fields, *J. Geophys. Res.*, *106*, 12,109–12,128, 2001.

Logan, J. A., Tropospheric ozone: Seasonal behavior, trends, and anthropogenic influence, *J. Geophys. Res.*, *90*, 10,463–10,482, 1985.

Logan, J. A., Trends in the vertical distribution of ozone: An analysis of ozonesonde data, *J. Geophys. Res.*, *99*, 25,553–25,585, 1994.

Logan, J. A., An analysis of ozonesonde data for the troposphere: Recommendations for testing 3-D models, and development of a gridded climatology for tropospheric ozone, *J. Geophys. Res.*, *104*, 16,115–16,149, 1999.

Luo, C., J. C. S. John, X. J. Zhou, K. S. Lam, T. Wang, and W. L. Chameides, A nonurban ozone air pollution episode over eastern China: Observations and model simulations, *J. Geophys. Res.*, *105*, 1889–1908, 2000.

Marenco, A., J. C. Medale, and S. Prieur, Study of tropospheric ozone in

the tropical belt (Africa, America) from STRATOZ and TROPOZ campaigns, *Atmos. Environ., Part A*, *24*, 2823–2834, 1990.
Martin, R. V., et al., Interpretation of TOMS observations of tropical tropospheric ozone with a global model and in situ observations, *J. Geophys. Res.*, *107*(D18), 4351, doi:10.1029/2001JD001480, 2002.
Marufu, L., F. Dentener, J. Lelieveld, M. O. Andreae, and G. Helas, Photochemistry of the African troposphere: Influence of biomass-burning emissions, *J. Geophys. Res.*, *105*, 14,513–14,530, 2000.
Mauzerall, D. L., D. Narita, H. Akimoto, L. Horowitz, S. Walters, D. Hauglustaine, and G. Brasseur, Seasonal characteristics of tropospheric ozone production and mixing ratios over East Asia: A global three-dimensional chemical transport model analysis, *J. Geophys. Res.*, *105*, 17,895–17,910, 2000.
McLinden, C. A., S. C. Olsen, B. Hannegan, O. Wild, M. J. Prather, and J. Sundet, Stratospheric ozone in 3-D models: A simple chemistry and the cross-tropopause flux, *J. Geophys. Res.*, *105*, 14,653–14,665, 2000.
Newell, R. E., and M. J. Evans, Seasonal changes in pollutant transport to the North Pacific: The relative importance of Asian and European sources, *Geophys. Res. Lett.*, *27*, 2509–2512, 2000.
Newell, R. E., E. V. Browell, D. D. Davis, and S. C. Liu, Western Pacific tropospheric ozone and potential vorticity: Implications for Asian pollution, *Geophys. Res. Lett.*, *24*, 2733–2736, 1997.
Oltmans, S. J., D. J. Hofmann, J. A. Lathrop, J. M. Harris, W. D. Komhyr, and D. Kuniyuki, Tropospheric ozone during Mauna Loa Observatory Photochemistry Experiment 2 compared to long-term measurements from surface and ozonesonde observations, *J. Geophys. Res.*, *101*, 14,569–14,580, 1996.
Oltmans, S. J., et al., Trends of ozone in the troposphere, *Geophys. Res. Lett.*, *25*, 139–142, 1998.
Pickering, K. E., A. M. Thompson, J. R. Scala, W. K. Tao, and J. Simpson, Ozone production potential following convective redistribution of biomass burning emissions, *J. Atmos. Chem.*, *14*, 297–313, 1992.
Poulida, O., R. R. Dickerson, and A. Heymsfield, Stratosphere-troposphere exchange in a midlatitude mesoscale convective complex, *J. Geophys. Res.*, *101*, 6823–6836, 1996.
Rood, R. B., A. R. Douglass, M. C. Cerniglia, and W. G. Read, Synoptic-scale mass exchange from the troposphere to the stratosphere, *J. Geophys. Res.*, *102*, 23,467–23,485, 1997.
Shun, C. M., and K. S. Leung, The first radioactivity and ozone soundings in Hong Kong, *Hong Kong Meteorol. Soc. Bull.*, *3*, 21–27, 1993.
Staehelin, J., J. Thudium, R. Buhler, A. Volz-Thomas, and W. Graber, Trends in surface ozone concentrations at Arosa (Switzerland), *Atmos. Environ.*, *28*, 75–87, 1994.
Staudt, A. C., D. J. Jacob, J. A. Logan, D. Bachiochi, T. N. Krishnamurti, and G. W. Sachse, Continental sources, transoceanic transport, and interhemispheric exchange of carbon monoxide over the Pacific, *J. Geophys. Res.*, *106*, 32,571–32,589, 2001.
Stohl, A., A 1-year Lagrangian "climatology" of airstreams in the Northern Hemisphere troposphere and lowermost stratosphere, *J. Geophys. Res.*, *106*, 7263–7279, 2001.
Stott, P., Savanna forest and seasonal fire in Southeast Asia, *Plants Today*, *1*, 196–200, 1988.
Thompson, A. M., The oxidizing capacity of the Earth's atmosphere: Probable past and future changes, *Science*, *256*, 1157–1165, 1992.
van Aardenne, J. A., G. R. Carmichael, H. LevyII, D. Streets, and L. Hordijk, Anthropogenic NO_x Emissions in Asia in the period 1990–2020, *Atmos. Environ.*, *33*, 633–646, 1999.
Volz, A., and D. Kley, Evaluation of the Montsouris series of ozone measurements in the nineteenth century, *Nature*, *332*, 240–242, 1988.
Wang, T., V. T. F. Cheung, K. S. Lam, G. L. Kok, and J. M. Harris, The characteristics of ozone and related compounds in the boundary layer of the South China coast: Temporal and vertical variations during autumn season, *Atmos. Environ.*, *35*, 2735–2746, 2001.
Wang, Y., D. J. Jacob, and J. A. Logan, Global simulation of tropospheric O_3-NO_x-hydrocarbon chemistry, 3, Origin of tropospheric ozone and effects of non-methane hydrocarbons, *J. Geophys. Res.*, *103*, 10,757–10,768, 1998.
World Meteorological Organization (WMO), Scientific assessment of ozone depletion, *Global Ozone Res. Monit. Proj. Rep. 37*, Geneva, 1994.
Ye, D., and G. Wu, The role of the heat source of the Tibetan plateau in the general circulation, *Meteorol. Atmos. Phys.*, *67*, 181–198, 1998.
Yeung, K. K., W. L. Chang, R. Newell, W. Hu, and G. L. Gregory, Tropospheric ozone profiles over Hong Kong, *Hong Kong Meteorol. Soc. Bull.*, *6*, 3–12, 1996.
Yienger, J. J., et al., The episodic nature of air pollution transport from Asia to North America, *J. Geophys. Res.*, *105*, 26,931–26,945, 2000.
Zhang, Y., K. R. Sperber, and J. S. Boyle, Climatology and interannual variation of the East Asian winter monsoon: Results from the 1979–95 NCEP/NCAR reanalysis, *Mon. Weather Rev.*, *125*, 2605–2619, 1997.

I. Bey and B. N. Duncan, EPFL-ENAC-LMCA, Lausanne Ch-1015, Switzerland. (isabelle.bey@epfl.ch; bryan.duncan@epfl.ch)
L. Y. Chan, Department of Civil and Structural Engineering, Hong Kong Polytechnic University, Hung Hom, Kowloon, Hong Kong, People's Republic of China. (celychan@polyu.edu.hk)
J. M. Harris and S. J. Oltmans, Climate Monitoring and Diagnostics Laboratory, NOAA, Mail Code R/CMDL, 325 Broadway, Boulder, CO 80303, USA. (joyce.m.harris@noaa.gov; samuel.j.oltmans@noaa.gov)
D. J. Jacob, R. V. Martin, and R. M. Yantosca, Department of Earth and Planetary Sciences and Division of Engineering and Applied Sciences, Harvard University, Pierce Hall, 29 Oxford Street, Cambridge, MA 02138, USA. (djj@io.harvard.edu; rvm@io.harvard.edu; bmy@io.harvard.edu)
H. Liu, NASA Langley Research Center, Mail Stop Chemistry and Dynamics Branch, Hampton,VA23681-2199,USA.(hyl@post.harvard.edu)

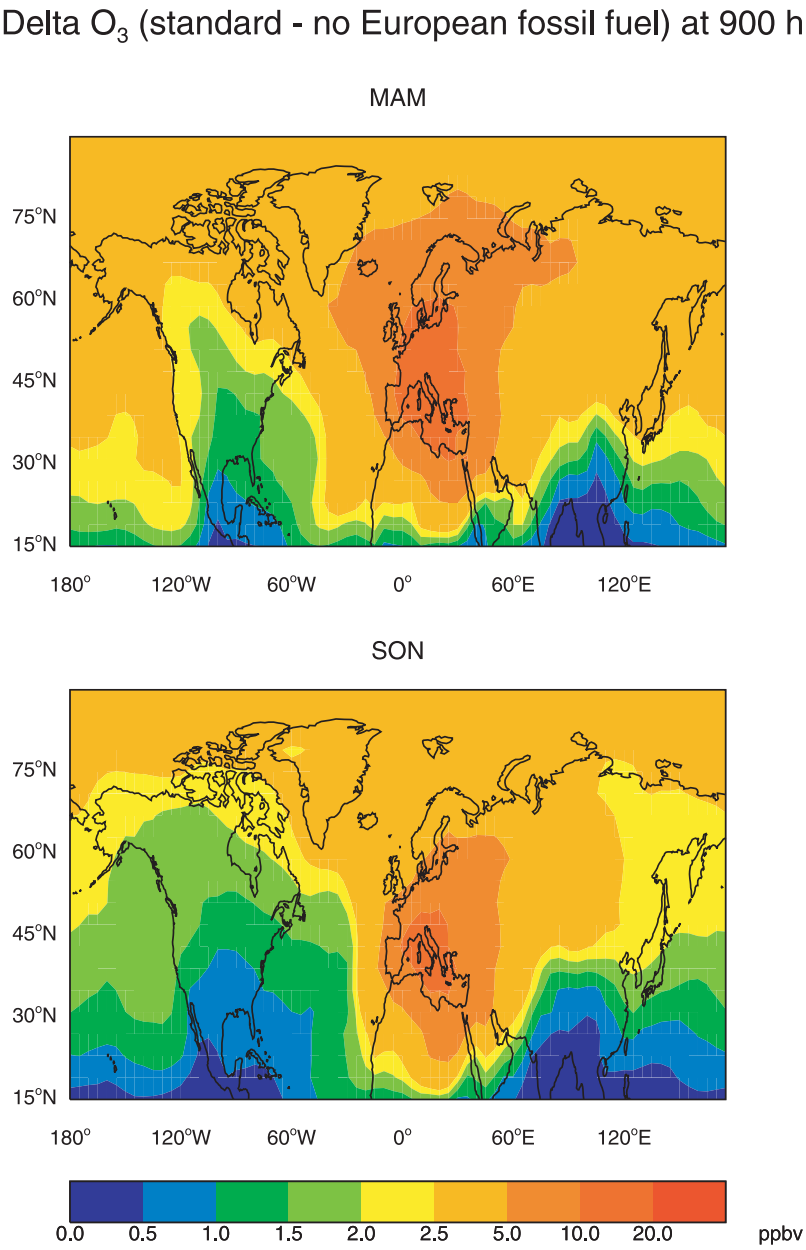

Figure 9. Decreases in ozone concentrations (ppbv) (a) at 900 hPa when European fossil fuel emissions are suppressed, (b) at 300 hPa when North American fossil fuel emissions are suppressed, relative to the standard simulation. Values are averages for spring (March–April–May) and fall (September–October–November) 1996.

(b) Delta O_3 (standard - no North American fossil fuel) at 300 hPa

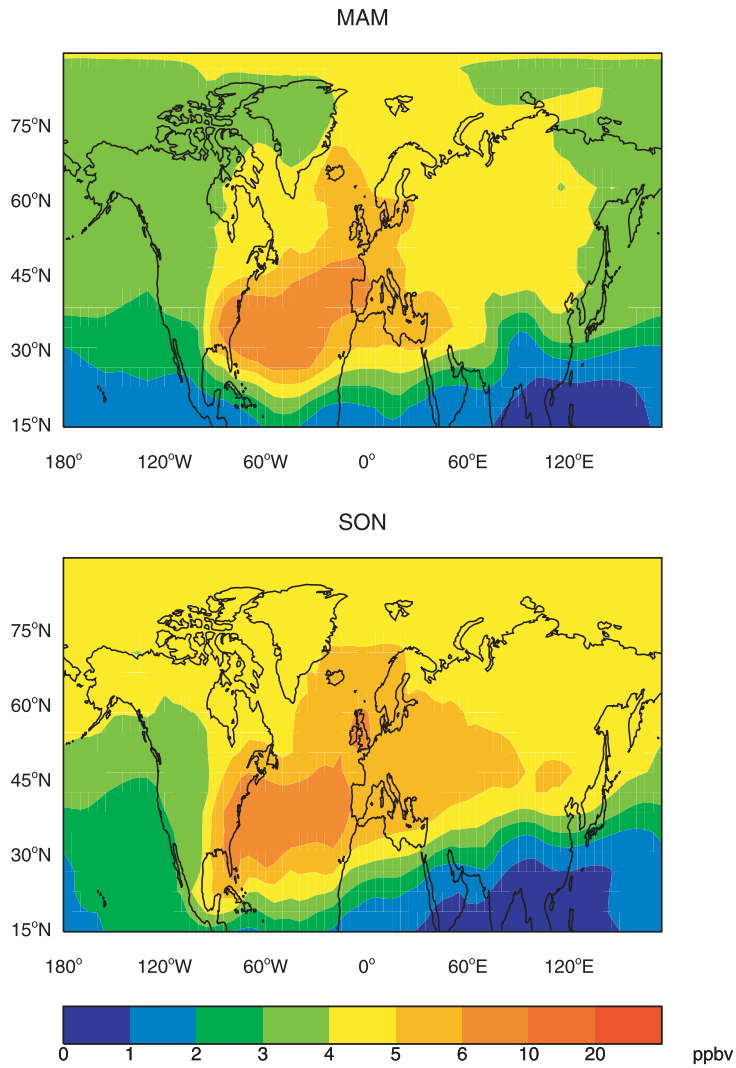

Figure 9. (continued)

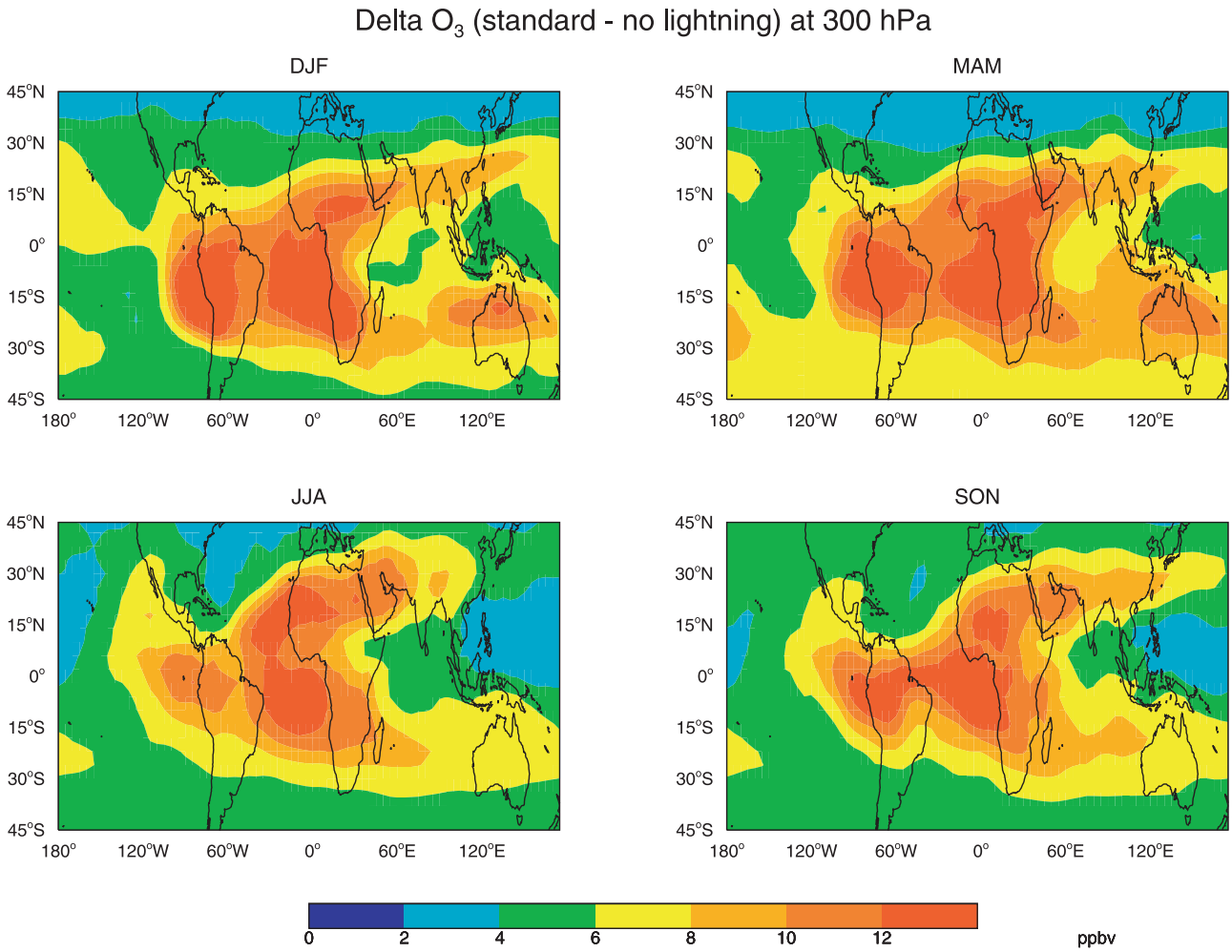

Figure 10. Decreases in ozone concentrations (ppbv) at 300 hPa when lightning NO_x emissions are suppressed, relative to the standard simulation for 1996. Values are seasonal averages for 1996.

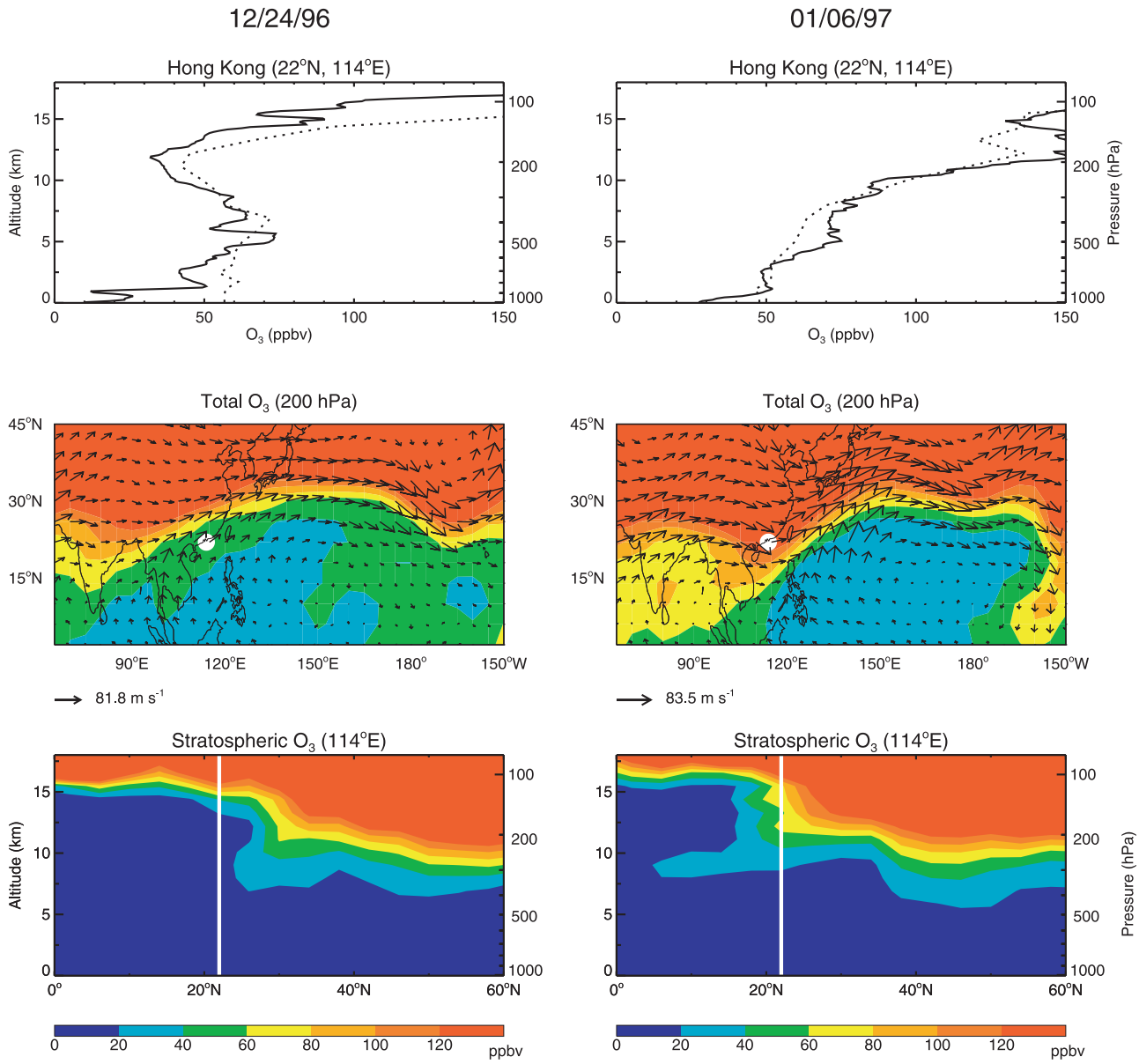

Figure 11. Case study illustrating the alternation between low and high ozone in the wintertime upper troposphere over Hong Kong. The top panels show ozonesonde profiles on December 24, 1996 and January 6, 1997. Observations (solid lines) are compared to model results for the corresponding days (dotted lines). The middle and bottom panels show additional model results for those days: (1) ozone concentrations and wind vectors at 200 hPa; (2) latitude-altitude cross-section at the longitude of Hong Kong (114°E) for the tagged ozone tracer originating in the stratosphere. The white dots and vertical lines correspond to the location of Hong Kong.

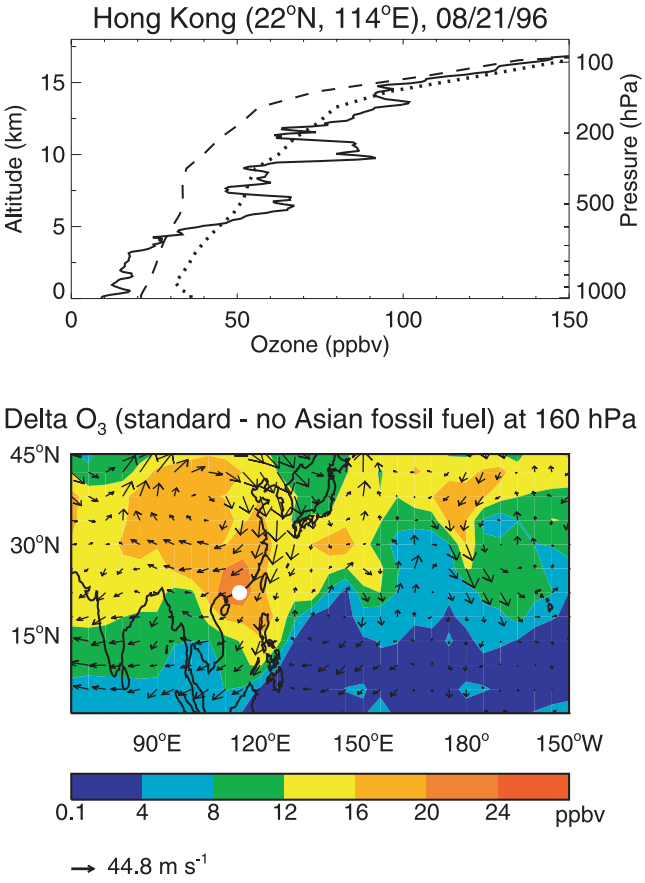

Figure 14. Summertime ozone pollution event in the upper troposphere over Hong Kong on August 21, 1996. The solid line shows ozonesonde observations, and the dotted line shows model results. Also shown as a vertical profile are simulated ozone concentrations when Asian fossil fuel emissions are suppressed (dashed line). The map shows decreases in ozone concentrations (ppbv) at 160 hPa (13 km), when Asian fossil fuel emissions are shut off, relative to the standard simulation. Arrows are wind vectors, and the white dot shows the location of Hong Kong.

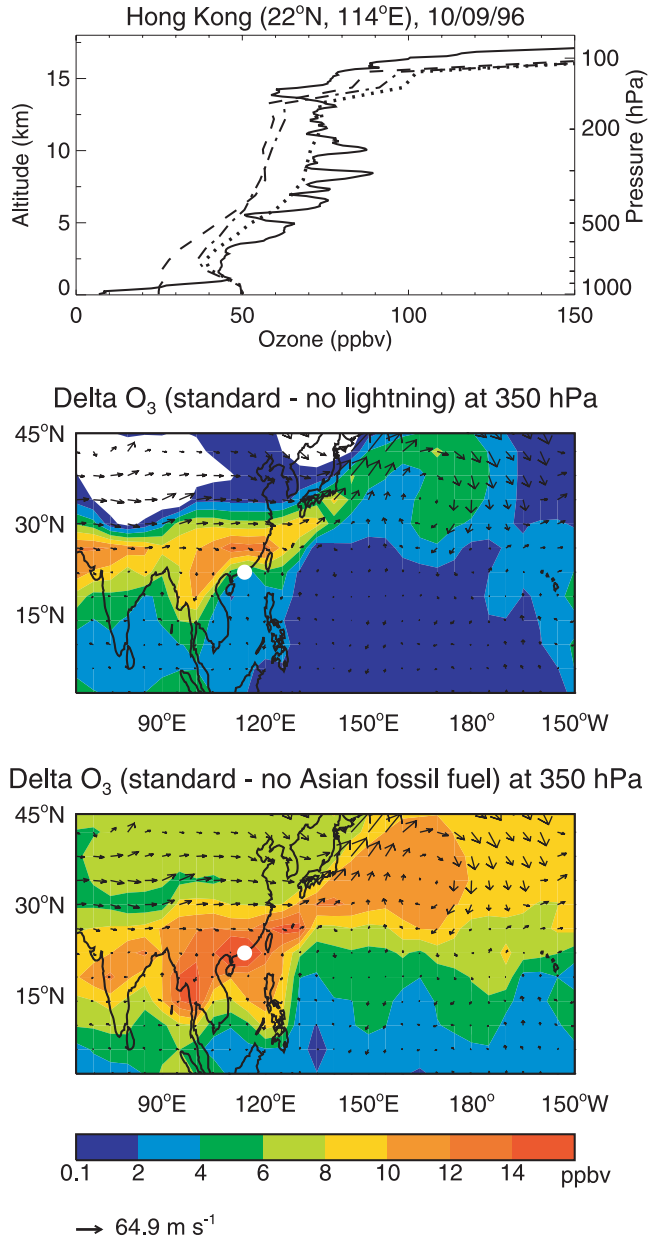

Figure 15. High-ozone episode over Hong Kong in fall (October 9, 1996). The solid line shows ozonesonde observations, and the dotted line shows model results (upper panel). Also shown as vertical profiles are ozone concentrations when lightning NO_x emissions (dash-dotted line) or Asian fossil fuel emissions (dashed line) are suppressed. Maps show decreases in ozone (ppbv) at 350 hPa (8 km) when lightning emissions (middle panel) or Asian fossil fuel emissions (bottom panel) are suppressed, relative to the standard simulation. Arrows are wind vectors, and the white dots show the location of Hong Kong.